

Organic Semiconductor Lasers

I. D. W. Samuel* and G. A. Turnbull

Organic Semiconductor Centre and Ultrafast Photonics Collaboration, SUPA, School of Physics and Astronomy, University of St Andrews, St Andrews, Fife KY16 9SS, U.K.

Received September 27, 2006

Contents

1. Introduction	1272
2. Materials	1273
2.1. Types of Organic Semiconductors	1273
2.2. Organic Semiconductor Photophysics	1274
2.3. Gain in Organic Semiconductors	1274
2.4. Comparison with Dyes and Inorganic Semiconductors	1276
3. Laser Resonators	1277
3.1. Generic Properties of Laser Resonators	1277
3.2. Microcavity Lasers	1278
3.3. Fabry–Perot Waveguide Lasers	1279
3.4. Microring and Microsphere Resonators	1280
3.5. Macroscopic Laser Resonators	1280
3.6. Diffractive Resonators	1281
3.6.1. One-Dimensional Distributed Feedback Resonators	1282
3.6.2. Two-Dimensional Distributed Feedback Resonators	1282
3.6.3. Three-Dimensional Distributed Feedback Resonators	1283
3.6.4. Photonic Design of Diffractive Organic Semiconductor Lasers	1283
3.7. Organic Semiconductor Laser Fabrication	1285
3.8. Resonator Conclusions	1285
4. Toward Applications of Organic Semiconductor Lasers	1285
4.1. Progress in Laser Operating Characteristics	1286
4.1.1. Output Power	1286
4.1.2. Temporal Characteristics	1286
4.1.3. Lifetime	1287
4.1.4. Spectral Properties	1287
4.1.5. Beam Properties	1287
4.2. Applications	1287
5. Future Developments	1289
5.1. Toward Electrical Pumping	1289
5.2. Indirect Electrical Pumping	1290
6. Conclusion	1291
7. References	1291

1. Introduction

The demonstration of the first laser, made with ruby in 1960,¹ has led to a revolution in science and technology. Lasers have transformed spectroscopy giving previously undreamed of insights into the physics and chemistry of the world around us, such as the direct observation of the

vibrations of chemical bonds.² They are used in a remarkable range of applications ranging from medicine to telecommunications. We now find them throughout everyday life in CD/DVD players, printers, and supermarket scanners.

Materials developments have played a crucial role in the development of new lasers. Organic semiconductors combine novel optoelectronic properties, with simple fabrication and the scope for tuning the chemical structure to give desired features, making them attractive candidates as laser materials, as well as for the other applications described in this issue. The rapid recent development of organic semiconductor lasers (OSLs) builds on the development of organic light-emitting diodes, which are now commercially available in simple displays. It opens up the prospect of compact, low-cost (even disposable) visible lasers suitable for applications from point of care diagnostics to sensing.

The development of organic transistors³ and light-emitting diodes (LEDs)^{4,5} came many years after their inorganic counterparts. In contrast, organic materials played a significant role in the development of lasers within a decade of the first laser. The broad spectra of organic molecules was exploited in dye lasers to give sources whose wavelength could be tuned, and lasers capable of short-pulse generation. In fact, the record for the shortest laser pulse was held until the 1990s by a dye laser based system.⁶ Dye lasers generally operated using dye solutions. Solid-state lasers using organic materials were demonstrated using dye-doped polymers in 1967,⁷ in doped single crystals in 1972,⁸ and on pure anthracene crystals in 1974.⁹ The growth of high-quality single crystals is demanding, and it is the much newer generation of easily processed organic semiconductors that opened up first the organic LED field^{4,5} and then the field of easily fabricated organic semiconductor lasers. The first of this wave of organic semiconductor lasers was reported in 1992 and consisted of a conjugated polymer in solution.¹⁰ Solid-state conjugated polymer lasers then followed in 1996^{11–14} and have been a topic of vigorous research since. In this review, we will focus on subsequent developments, with particular emphasis on the period since 1999–2001, when a number of very useful reviews appeared.^{15–19} We consider a wider range of materials than previous reviews, most of which focused either on conjugated polymers^{15,17–20} or small molecules,¹⁶ and conclude with the recent breakthrough of direct diode pumping of organic semiconductor lasers.

A laser consists of a material capable of amplifying light in a cavity (or resonator), which applies feedback. The amplification occurs by the process of stimulated emission, illustrated schematically in Figure 1. An incident photon stimulates a transition between the excited state and ground



Ifor Samuel is Professor of Physics and Director of the Organic Semiconductor Centre at the University of St Andrews. He was born in London and later received his first degree and Ph.D. from the University of Cambridge, working on optical spectroscopy of organic semiconductors. He was a Research Fellow at Christ's College, Cambridge, and also performed postdoctoral work at CNET-France Telecom in Paris. He was awarded a Royal Society University Research Fellowship in 1995 and moved to Durham to set up his own research group. He moved to Scotland to take up his current position seven years ago and has recently been awarded a Senior Research Fellowship by the Engineering and Physical Sciences Research Council. He is a Fellow of the Royal Society of Edinburgh and of the Institute of Physics. His research is focused on the physics of organic optoelectronic materials and devices.



Graham Turnbull was born in Edinburgh, Scotland, in 1973 and brought up in the Scottish Borders. He graduated with a first-class M.Sc. degree in physics in 1995 and a Ph.D. in 1999, both from the University of St Andrews. His doctoral research project, on the topic of continuous-wave optical parametric oscillators, was supported by a Carnegie Trust Scholarship. He joined the polymer optoelectronics group at the University of Durham as a postdoctoral researcher in 1999 and, after a brief period in Durham, returned to St Andrews, where he is currently a lecturer in the School of Physics and Astronomy. Since 2002, he has also held an EPSRC Advanced Research Fellowship for research into advanced solid-state polymer laser systems. His current research interests include polymer photonics, nonlinear optics, soft lithography, and optofluidics.

state of the medium, generating further photons. The crucial point about stimulated emission is that the additional photons have the same phase as the incident photon, and this leads to the distinctive coherence of the emitted light, so laser beams can have extremely well-defined frequency and very small divergence. The remainder of the article discusses organic semiconductor materials for lasers, followed by resonator design, fabrication, progress toward applications, and future challenges.

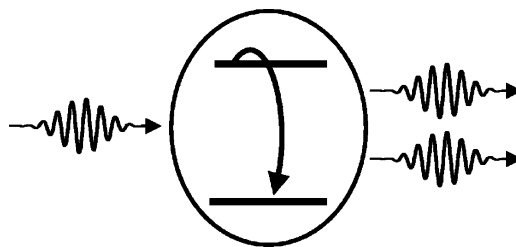


Figure 1. Schematic illustration of the stimulated emission process. An incoming photon interacts with a chromophore in an excited-state to stimulate the emission of a second photon in phase with the first.

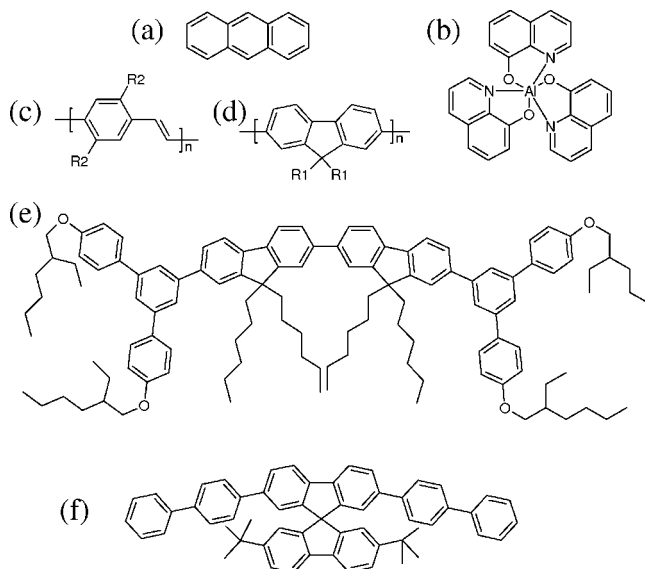


Figure 2. Chemical structures of typical organic semiconductors used for lasers: (a) anthracene; (b) aluminum tris(quinolate); (c) generic poly(*para*-phenylene vinylene) derivative; (d) generic polyfluorene derivative; (e) bisfluorene cored dendrimer; (f) spiro-linked oligomer.

2. Materials

2.1. Types of Organic Semiconductors

There are several types of organic semiconductors relevant to lasing, and their classification is by a combination of structural features and how they are processed. Organic semiconductors are conjugated molecules, with the semiconducting properties arising from the overlap of molecular orbitals. Early work focused on single crystals of materials such as anthracene,⁹ Figure 2a. When sufficiently high voltages were applied, light was emitted, but the difficulties of growing and handling these materials meant that it was the discovery by Tang and Van Slyke of efficient electroluminescence in evaporated films of small molecule organic semiconductors that attracted serious interest in using the materials for light emission.⁴ We will refer to this class of organic semiconductor as small molecules, and an example is aluminum tris(quinolate) (Figure 2b).

There are three other types of organic semiconductors that have been studied as laser materials. The first is conjugated polymers. These long chain-like molecules have alternating single and double bonds giving electron delocalization along the molecule. Two families of conjugated polymer have been studied particularly extensively: the poly(phenylene vinyl-

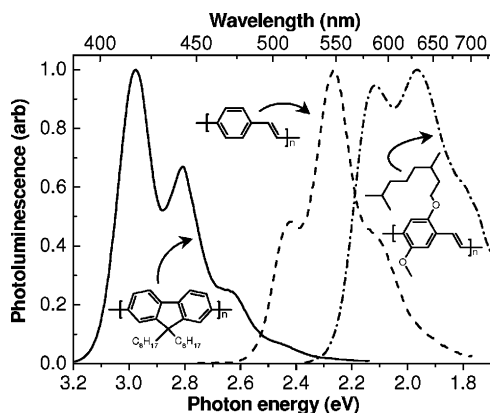


Figure 3. Fluorescence spectra of three conjugated polymers typical of those used for lasers with chemical structures shown as insets.

ene)s^{11,14,21–32} (Figure 2c) and the polyfluorenes^{33–37} (Figure 2d). A major difference from small molecules is that conjugated polymers can be deposited from solution by processes such as spin-coating and ink-jet printing, giving even simpler fabrication of devices. Two further types of organic semiconductor have been studied for lasers (and LEDs). The first of these is conjugated dendrimers.³⁸ These typically consist of a chromophore at the core, conjugated branches (dendrons), and surface groups.^{39–41} The core defines the key electronic properties such as the color of light emission, while the surface groups confer solubility. The highly branched structure contrasts with the much more linear structure of conjugated polymers. An example of a conjugated dendrimer is shown in Figure 2e. The material shown is a first generation dendrimer, so it has just one level of branching. It consists of a bisfluorene core with meta-linked biphenyl dendrons and ethylhexyloxy surface groups. Dendrimers with nonconjugated dendrons and laser dyes incorporated into a dendritic host have also been studied for lasing and amplification.^{42,43} Another type of organic semiconductor is the spiro-compounds.^{44–47} These consist of two oligomers coupled to each other by a spiro linkage, and an example is shown in Figure 2f.

2.2. Organic Semiconductor Photophysics

There are many aspects of the photophysics of organic semiconductors that are relevant to lasers. First, the materials absorb light very strongly, so at the peak of the absorption spectrum, a thin film only 100 nm thick can absorb 90% of the light incident on it. This means that light can be absorbed in very short distances and, since stimulated emission is closely related to absorption, also means that very strong gain is also possible. Both attributes have been demonstrated very clearly in Tessler's work showing lasing using a conjugated polymer film only 100 nm thick.¹¹ The strong absorption and gain have a major impact on resonator design, which is discussed in section 3. The fluorescence spectra of organic semiconductors are broad and, in addition, can be tuned by changing the chemical structure to give light emission across the visible spectrum and into the near ultraviolet and infrared. The broad spectra and scope for color tuning are illustrated in Figure 3, which shows the fluorescence spectra of three common conjugated polymers. The broad spectra mean that organic semiconductor lasers can be tuned over a significant spectral range^{35,48–53} and also mean that these materials are capable of short pulse generation^{54,55} and broad-band optical amplification.^{56,57}

For both LEDs and lasers, it is desirable to use materials that emit light efficiently. The efficiency of light emission can be described quantitatively by the photoluminescence quantum yield (PLQY), which is defined as the ratio of the number of photons emitted by a sample to the number of photons absorbed. For thin films of organic materials, it can be conveniently measured by placing a thin film in an integrating sphere, which collects the light emitted in all directions.^{58–61} Considerable effort has gone into increasing the photoluminescence efficiency of thin films of organic materials. In particular, a range of strategies have had to be developed to control intermolecular interactions. At high concentrations or in the solid state, conjugated organic molecules can interact with their neighbors, leading to the formation of (physical) dimers, aggregates, or excimers, which can quench light emission.⁶² Hence many laser dyes, which are extremely fluorescent materials in dilute solution, are almost nonemissive in the solid state.

Clearly, most applications of organic semiconductors involve their use in the solid state. The approaches to avoiding quenching generally involve increasing the spacing of the chromophores (light-emitting units). For small molecules, this is frequently done by blending with a host material.⁶³ In conjugated polymers, bulky side groups are often used to confer solubility and to keep the polymer chains apart.^{22,64} Light-emitting dendrimers have been designed with the chromophore at the core and the dendrons acting as spacers.^{40,41,65} In the spiro compounds, the spiro linkage imposes a geometry that makes dense packing of the chromophores difficult, thereby controlling the intermolecular interactions.^{44,46,66}

2.3. Gain in Organic Semiconductors

A laser consists of a medium capable of amplifying light (known as the gain medium) in a resonator. In this subsection, we will consider the origin and properties of the gain in organic semiconductors, while the effect of the resonator will be discussed in the next section. When a photon is incident on a material, it can cause an electron to be excited from a lower to a higher energy level, the process we know as absorption. Similarly, when a photon is incident on a material that has already been excited, it can cause an electron to fall from a higher to a lower energy level and the emission of another photon. This process is known as stimulated emission, and its existence was first proposed by Einstein based on thermodynamic considerations. Further information about this discovery and laser physics can be found in countless lasers textbooks including those of Siegman⁶⁷ and Svelto.⁶⁸ A crucial point is that the photon emitted has the same phase, frequency, and direction as the incident photon. The fact that an additional photon is released means that there has been amplification of the incident photon. So as light travels through a gain medium, it stimulates the emission of more and more photons and (for small signals) its intensity, $I(z)$, increases exponentially with distance:

$$I(z) = I(z=0) \exp(gz) \quad (1)$$

where g is the wavelength-dependent gain coefficient of the medium. Einstein showed that for a particular transition, the cross sections for absorption and stimulated emission are the same. This means that in order to get more stimulated emission than absorption at a given wavelength, we need to

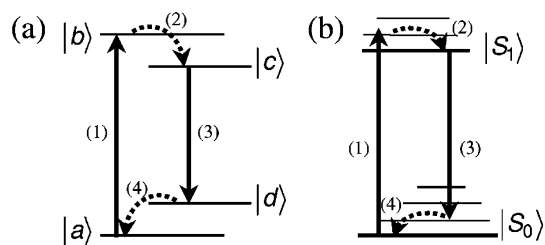


Figure 4. Energy level diagrams for optical gain media: (a) energy levels and transitions of a generic four-level laser material—transitions 1 and 3 are optical absorption and emission, and transitions 2 and 4 are thermal relaxations; (b) energy levels of the lowest two singlet states in an organic semiconductor, including the corresponding optical and thermal transitions to those in panel a.

have more molecules excited to the upper state than are in the lower state, a situation known as a population inversion. The gain coefficient is simply the product of the stimulated emission cross section, σ , and the population inversion density, N , that is, $g = \sigma N$. Inversion cannot be practically achieved in a system with just two energy levels. However, it can be achieved in a system with three or four energy levels.

A four-level system is shown in Figure 4a. Light excites a molecule from the ground state to an excited state (transition 1 in the figure), and it then rapidly relaxes to another energy level (transition 2). The lasing transition (3) then occurs down to a fourth level, which is above the ground state. There is then a rapid return to the ground state via transition 4. The advantage of a four-level system such as this is that there can be a population inversion between levels $|c\rangle$ and $|d\rangle$, even when most molecules are in the ground state, so lasing can be obtained for a very low rate of excitation, that is, the threshold for lasing is low.

The energy levels in a typical organic semiconductor are shown in Figure 4b. The figure shows the ground state and first excited singlet state. Each of these electronic energy levels is subdivided into vibronic sublevels. The spacing of these sublevels is approximately 0.2 eV, so at room temperature, there is little thermal excitation from the lowest level. Light can excite the molecule from its ground state to an excited vibrational level of the singlet manifold (corresponding to transition 1 in Figure 4a). This will be followed by rapid vibrational cooling to the bottom of the singlet manifold (transition 2). Lasing can then take place by transition 3 to a vibrationally excited level of the ground-state manifold, followed by vibrational relaxation (transition 4). Hence the energy levels of organic semiconductors enable them to behave as four-level lasers, with associated low thresholds. It also explains why the emission occurs at longer wavelength than the absorption.

There is an additional factor that contributes to separating the absorption and emission, especially in the solid state. In a film of an organic semiconductor, there will be a distribution of environments and hence a distribution of energy levels. This is particularly the case in conjugated polymers, which can have a great deal of conformational disorder, giving segments with a range of energy levels. We can regard the sample as consisting of many different sites of different energy. We initially excite molecules or segments of molecules with a wide range of site energies, but energy is rapidly transferred to the lowest energy molecules or segments. This has been elegantly described in terms of a

Gaussian disorder model by Bässler's group,^{69,70} and the associated red shift of emission as a function of time has been observed experimentally.^{71–74} Importantly, much of the shift occurs in the first few picoseconds after excitation (though, of course, the dispersive nature of the process means that it continues over many orders of magnitude of time). This energy-transfer process means that emission occurs from the lowest energy sites in the sample and so increases the separation between absorption and fluorescence. This in turn is helpful for lasing because it reduces the amount of absorption at the lasing wavelength. The separation between absorption and emission can be increased further by blending two different materials with different energy gaps. Light absorbed by the wider energy gap material will lead to energy transfer to the lower energy gap material and emission from that material. One example is the use of a blend of the red laser dye 4-(dicyanomethylene)-2-methyl-6-(4-dimethylaminostyryl)-4H-pyran (DCM) as a dopant in the green host material tris(8-hydroxyquinoline) aluminum (Alq_3).^{75,76} Another example is green-emitting polymers in a blue host.^{25,77} The energy transfer process has been studied and been shown to be by the Förster mechanism.^{78–80} A closely related way of separating the emission from the absorption is to use a copolymer consisting of wider and narrower energy gap segments, and this has been demonstrated successfully for lasers^{81,82} and optical amplifiers.⁵⁶

The presence of gain in a material is an essential condition for it to be possible for lasing to occur. There have been two main approaches to studying gain in potential organic semiconductor laser materials. The first is by transient absorption measurements. The second is by measurements of amplified spontaneous emission (ASE). Transient absorption measurements are an all-optical approach to ultrafast measurements of photoexcitations. The sample is excited by a short pump pulse, which generates photoexcitations, and a time-delayed probe pulse is then used to measure the resulting change in transmission of the sample due to the formation of the photoexcitations. By changing the time-delay between the pump and probe pulses, one can measure the transmission as a function of time with a time-resolution comparable to the duration of the laser pulses used (typically 100 fs). The newly formed photoexcitations absorb in some parts of the spectrum, while in other parts of the spectrum there is a reduction of absorption (bleaching) due to the reduced population in the ground state. If there is gain in the sample, the probe will be amplified by stimulated emission and be stronger after passing through the sample. Hence transient absorption provides a powerful means for studying photoexcitations and their time evolution, together with gain and its time evolution. An example of such a measurement is shown in Figure 5. The decrease in absorption from 1.8 to 2.15 eV is mainly due to stimulated emission. The graph therefore shows the spectral and temporal evolution of gain, including the red shift with time mentioned in the previous paragraph. There are three main factors that determine the overall gain spectrum. They are the gain spectrum of the material, the ground-state absorption, and excited-state absorption. The overall gain is the material gain minus absorption.

Early work toward making conjugated polymer lasers involved making transient absorption measurements on members of the poly(*p*-phenylene vinylene) family of polymers.^{83,84} In the first of these studies, no gain was observed, probably due to the material used or the excitation

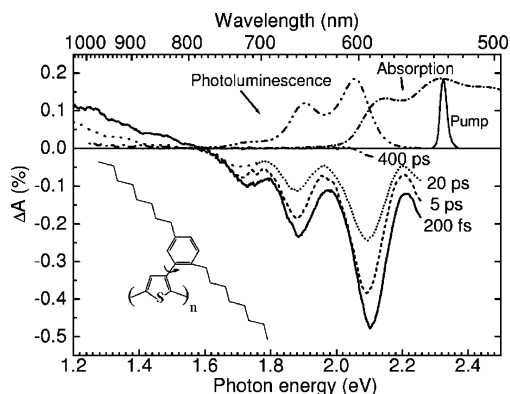


Figure 5. Transient absorption spectra of poly[3-(2,5-dioctylphenyl)-thiophene]; chemical structure inset. Reprinted from *Journal of Luminescence*, vol. 76 and 77, A. Ruseckas, M. Theander, L. Valkunas, M. R. Andersson, O. Ing nas, and V. Sundstr m, “Energy transfer in a conjugated polymer with reduced interchain coupling”, pp 474–477, Copyright 1998 with permission from Elsevier.

wavelength (310 nm). In the other study, the gain was extremely short-lived, and this was attributed to the rapid formation of intermolecular photoexcitations with strong photoinduced absorption overlapping the gain. In subsequent work, with improved materials, there have been numerous reports of gain in organic semiconductors and its dynamics.^{24,74,85–88} These studies have confirmed that very high gain is possible. They have also shown that gain lifetimes are usually short, on the picosecond time scale. This presents a challenge for lasers, because a short excited-state lifetime means that a high pump rate is needed to maintain a population inversion. However, too high a pump rate leads to exciton–exciton annihilation, which is an undesirable nonradiative decay process.

The other main method for measuring gain is by ASE. This involves making a slab waveguide of an organic semiconductor, exciting it with pulsed pump-laser light in a stripe near the edge of the sample, and looking at the light emitted from the edge of the sample. Some of the light emitted by the material is waveguided along the length of the excitation stripe. This guided spontaneous emission can be amplified by stimulated emission before being emitted from the edge of the film. Light at the peak of the gain spectrum of the material will be amplified more than other light, leading to a spectrally narrowed emission (typically a few nanometers full width at half-maximum) above a particular pumping intensity. The change in spectral shape with excitation density is illustrated in Figure 6.

In the case of ASE, spontaneous emission within the film acts as the “probe pulse”. One must therefore use an indirect method to measure the gain of the material. The wavelength-dependent output intensity, $I(\lambda)$, of the ASE is given by the relationship

$$I(\lambda) = \frac{A(\lambda)I_p}{g(\lambda)}[\exp(g(\lambda)l) - 1] \quad (2)$$

where $A(\lambda)$ is a constant related to the emission cross section, I_p is pumping intensity, and l is the length of the stripe. So, by monitoring the intensity of the line-narrowed emission as a function of the stripe length, one may calculate the net gain, $g(\lambda)$. This method was initially applied to the inorganic semiconductor cadmium sulfide⁸⁹ but has since been widely applied to determine the gain of organic semiconductors.^{35,90–92} Additionally, by progressively moving the stripe away from

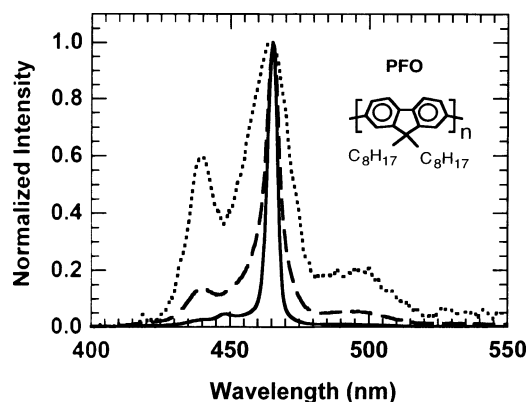


Figure 6. The change in spectral shape with increasing excitation density of the edge emission from a PFO film. The normalized spectra show a significant spectral gain narrowing at high excitation densities. Reprinted with permission from *Applied Physics Letters*, vol. 81, G. Heliotis, D. D. C. Bradley, G. A. Turnbull, and I. D. W. Samuel, “Light amplification and gain in polyfluorene waveguides”, pp 415–417, Copyright 2002 American Institute of Physics.

the edge of the film, it is possible to measure the waveguide losses of light propagating through an unpumped region of the film. Waveguide losses in conjugated polymers typically lie in the range of 3–50 cm^{-1} , with the lower end of the range being for copolymers. Even lower losses ($<1 \text{ cm}^{-1}$) have been reported in blended organic thin films.⁹³ Net gains have been measured for a wide range of materials and can be over 60 cm^{-1} at modest pumping densities of 4 kW cm^{-2} .⁹¹ Measurements of ASE are generally very useful because they are relatively simple to perform and the geometry is close to that used in waveguide lasers. However, transient absorption gives more insight into the factors controlling the gain, can readily probe the entire emission spectrum, and gives the gain dynamics. The high gain of organic semiconductors has several consequences: very compact lasers can be made, the lasers are tolerant of minor fabrication defects, and the materials can also be used to make compact optical amplifiers (section 4.2).

2.4. Comparison with Dyes and Inorganic Semiconductors

Readers familiar with laser dyes will have noticed some similarities between dyes and organic semiconductors, and it is useful to compare and contrast the two classes of material. The main similarities are that both classes of material have broad spectra, can be tuned across the visible spectrum (and beyond) by changing the structure, and behave as quasi-four-level laser materials. There are, however, some important differences. One is that organic semiconductors can have high photoluminescence quantum yield even as neat films in the solid state. In contrast, dyes need substantial dilution to give high solid-state quantum yields. This gives organic semiconductors scope to offer stronger pump absorption and gain than dyes in the solid state. Another difference is that many organic semiconductors offer the scope for simple processing to make thin film laser structures, for example, by solution processing. A further difference from dyes is that organic semiconductor films are capable of charge transport, opening up the possibility of electrical pumping in the future.

It is also interesting to compare organic and inorganic semiconductors. Similarities are that they can both give

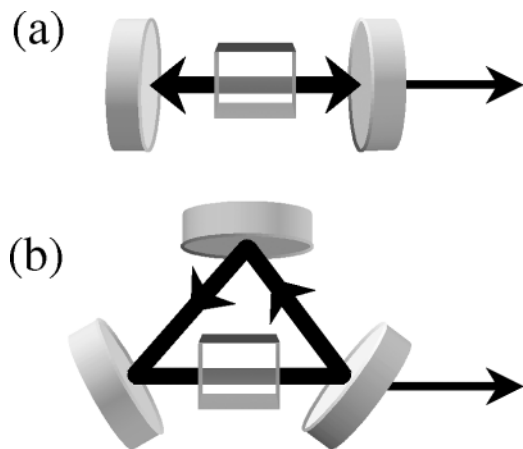


Figure 7. Schematic diagrams of generic laser resonator structures: (a) linear Fabry–Perot cavity, with gain medium located between two parallel mirrors, supporting a standing-wave resonant light field; (b) three mirror ring cavity, supporting a traveling-wave resonant light field through the gain medium.

efficient light emission in the solid state and that they are both capable of charge transport. There are however, numerous differences. The organic semiconductors currently of interest for lasers are much more disordered than their inorganic counterparts, giving much lower mobility. Exciton binding energies in organic semiconductors are very much larger (~ 0.5 eV), so their excitons are strongly bound even at room temperature. The localized excited states in organic semiconductors mean that there is little dependence of the threshold on temperature, in contrast to inorganic semiconductors.⁹⁴ In general, organic semiconductor excited-state lifetimes of up to around a nanosecond are shorter than those in inorganic semiconductors. In the case of organic semiconductors, there is a very wide range of materials with visible band gaps. However, the greatest difference is probably the scope for simple fabrication of organic semiconductor devices by simple techniques such as evaporation and ink-jet printing.

3. Laser Resonators

3.1. Generic Properties of Laser Resonators

As mentioned in the introduction, every kind of laser consists of two basic elements. First there is an optical gain medium that amplifies the light via stimulated emission and second an optical feedback structure that repeatedly passes a resonant light field through the gain medium to establish a very intense, coherent optical field inside the laser. This optical feedback system is conventionally called the optical resonator or optical cavity. In the very simplest case, this optical cavity may comprise only two mirrors, configured as a Fabry–Perot interferometer, between which the amplifying gain medium is situated (Figure 7a). This Fabry–Perot-type resonator is the simplest example of a linear cavity that supports a standing-wave optical field between the two mirrors. A second simple configuration for an optical cavity is an optical ring resonator, in which the light circulates as a travelling wave around a closed path defined by three or more mirrors (Figure 7b).

There are many variations of these two basic cavity structures,^{67,68} but they ultimately all impose two basic properties upon the oscillating laser light field. First, they define the allowed resonant frequencies of the device (within

the constraint of the gain medium's emission spectrum) and hence the wavelengths of the laser field. Second, they define the spatial characteristics of the laser beam that is output from the resonator. These defining characteristics of the laser light arise from the fundamental boundary condition of the laser field: the laser light field must be unchanged in both amplitude and phase following one round-trip of the optical cavity. This requirement leads to a discrete set of resonant frequencies for a given laser resonator, each of which must have an integer number of optical cycles, or wavelengths, in one round-trip of the cavity. These frequencies are known as the longitudinal, or axial, modes of the resonator. The optical cavity will also define certain transverse mode patterns that are self-replicating following a round trip of the structure. These transverse modes within the laser cavity ultimately determine the transverse light pattern of the emitted laser beam.

The cavity is also key to the power characteristics of the laser and has an impact on both the oscillation threshold and the output efficiency. To achieve a sustained oscillation in a laser, amplification in the gain medium must (at least) balance out with the optical loss (dissipation) during each round-trip of the cavity. The intensity of light passing through a gain medium of length l is amplified by a factor $\exp(\sigma Nl)$. The magnitude of the population inversion density, and hence the gain, depends on the external pumping rate. In the case of steady-state optical pumping, $N = P_p \tau / (h\nu V)$, where, P_p is the pump power, τ is the excited-state lifetime, $h\nu$ is the pump photon energy, and V is the volume of the population inversion. For pulsed optical pumping, with a pump pulse of energy E_p and a duration much less than the excited-state lifetime, the initial excitation density is $N(t=0) = E_p / (h\nu V)$ and decays away with time due to spontaneous and stimulated emission and various nonradiative decay paths. The optical loss in the resonator, meanwhile, is due to a product of transmission losses through each of the mirrors and any other absorption and scattering losses in the cavity components. The round-trip fractional optical loss β may therefore be written as

$$\beta = 1 - \exp(-\gamma) \prod R_i \quad (3)$$

where R_i is the reflectivity of the i th mirror in the cavity and γ is a loss coefficient embodying all scattering and absorption losses.

Thus as light propagates round a ring laser resonator, its intensity will change by a factor $\exp(\sigma Nl) \exp(-\gamma) \prod R_i$ in each round trip. (For a linear laser resonator the intensity will change by a factor $\exp(2\sigma Nl) \exp(-\gamma) \prod R_i$, due to the double pass through the gain medium in each round trip.)

If the pumping rate is too low, then the gain from stimulated emission cannot exceed the round-trip loss, and a light field cannot build up in the laser cavity. In this case, the excitations in the gain medium are radiated in all directions as spontaneous emission. At a certain critical pumping rate, known as the threshold rate, the gain balances out the round-trip losses, and

$$\exp(\sigma N_{\text{TH}} l) \exp(-\gamma) \prod R_i = 1 \quad (4)$$

where N_{TH} is the excitation density at threshold. When the pump rate increases beyond this value, a coherent light field will grow inside the laser cavity. Some of this light will leak out as an intense coherent laser beam whose power will rise linearly with the excess pump rate. The lower the loss of

the optical cavity, therefore, the lower will be the optical gain required to make the laser oscillate. Low-loss resonators are therefore very attractive for achieving lasing for modest external pumping rates.

The striking change in operation around the lasing threshold can be understood by considering the many “photon modes” into which light may be emitted.⁶⁷ Below threshold there may be $\sim 10^6$ to 10^{10} spectral and spatial modes into which the light may be emitted. That is it may be emitted into a wide range of different spatial directions and different wavelengths. As the pump excitation increases, the probability of finding a photon in any one of these modes at a given time rises. The lasing threshold occurs when one of these modes (the one with the lowest cavity losses) exceeds an average of one photon in it at all times. When pumping above this threshold, the stimulated emission into this one mode rapidly builds up to dominate spontaneous emission into all of the others, and the excess pumping energy is efficiently converted into a coherent laser field.

Independent of this requirement for lasing threshold, the resonator also affects the output efficiency of a laser. When pumped above threshold, the output power, P_{out} , from a laser varies with pump power, P_{p} , as

$$P_{\text{out}} = \frac{T_{\text{out}} \lambda_{\text{p}}}{\beta \lambda} \eta_{\text{PL}} (P_{\text{p}} - P_{\text{pTH}}) \quad (5)$$

In eq 5, λ and λ_{p} are the wavelengths of the laser and optical pump source, η_{PL} is the emission efficiency of the optical gain medium (when under strong excitation), T_{out} is the transmission of a partially reflecting output-coupling mirror, and P_{pTH} is the pump power at threshold. Output efficiencies from a laser are usually expressed as a power slope efficiency, which is the differential efficiency of output power to pumping power, $\eta_{\text{PL}} \lambda_{\text{p}} T_{\text{out}} / (\lambda \beta)$. Clearly several factors affect the slope efficiency, including the emission efficiency of the gain medium. But one easily engineered parameter is the ratio of useful output-coupling losses to the total round-trip losses of the cavity. In order to have a highly power-efficient laser, one requires that the useful output-coupling losses form a very large fraction of the total losses of the resonator. These total losses may include absorption, scattering, and unwanted transmissions of the resonant light field. In order to optimize the power characteristics of the laser, one would therefore choose to have as low a loss or high-quality optical cavity, of which as great a fraction of the loss as possible is due to an element that extracts a useful output beam from the intracavity light field.

Laser resonators are, of course, often much more complicated than the very simple generic linear and ring cavities shown in Figure 7 and may contain many other elements.⁶⁸ Notably there may be other structures that provide additional wavelength selection, control of the polarization state or transverse mode, or even switching elements that may modulate the losses of the resonator. For lasers based on very broad-band gain media, such as organic molecules, it is common to include a highly dispersive element such as a diffraction grating, which will introduce additional substantial losses for all but a narrow band of wavelengths.⁹⁵ By changing the properties or orientation of this dispersive element, one may tune the narrow wavelength band that experiences low loss and hence tune the laser emission throughout the wide gain bandwidth of the gain medium.

Optically pumped organic semiconductor lasers have been demonstrated in a very wide variety of different resonant

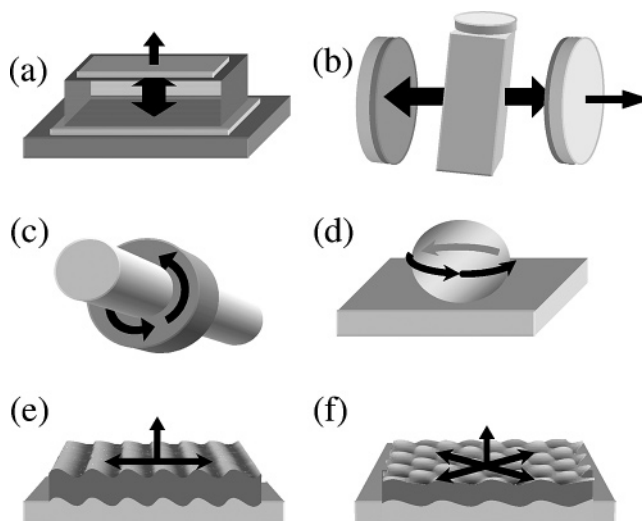


Figure 8. Schematic resonators used for organic semiconductor lasers showing propagation directions of the resonant laser field: (a) planar microcavity; (b) Fabry–Perot dye laser cavity; (c) microring resonator, coated around an optical fiber; (d) spherical microcavity; (e) distributed feedback resonator; (f) 2D DFB/photonic crystal resonator.

structures. These include the “conventional” laser cavities described above, although most work has concentrated on microscopic resonators based on thin films of the organic semiconductor. Organic lasers configured as planar, cylindrical, and spherical microcavities, optical waveguide based cavities, and a remarkable range of diffractive structures have been studied, some of which are illustrated in Figure 8. While some of these appear quite different from the generic cavities shown in Figure 7, their basic function, in providing resonant feedback through the gain medium, is fundamentally the same. The different geometries of these lasers, however, lead to a rich variety of spectral, spatial, and power properties. In the rest of this section, we will discuss the properties of OSLs grouped by the resonator type and discuss progress in designing and fabricating novel feedback structures.

3.2. Microcavity Lasers

Building on the successful development of organic semiconductor LEDs, which consist of a planar sandwich of the organic material between two conducting contacts, perhaps the most natural initial cavity arrangement for a solid-state organic semiconductor laser was the planar microcavity. Tessler and co-workers were first to demonstrate an optically pumped organic microcavity laser in 1996.¹¹ The structure of their laser is illustrated in Figure 8a. It consisted of a 100 nm thick layer of poly(*para*-phenylene vinylene) (PPV) between a pair of mirrors. The laser was fabricated by spin-coating the polymer film onto a broad band, highly reflecting dielectric mirror, and then a second partially transmitting silver mirror was deposited on top of the polymer. This structure is essentially the same as the basic linear cavity illustrated in Figure 7a and was designed to support a standing-wave optical field between the two mirrors. As mentioned above, this kind of cavity supports a discrete set of wavelengths such that twice the optical length of the resonator is equal to an integer number of wavelengths. This particular laser supported three resonant modes between 500 and 600 nm. Below threshold, the spontaneous emission was emitted almost equally into each optical mode. However, above a pulsed optical pump energy of ~ 100 nJ (pump

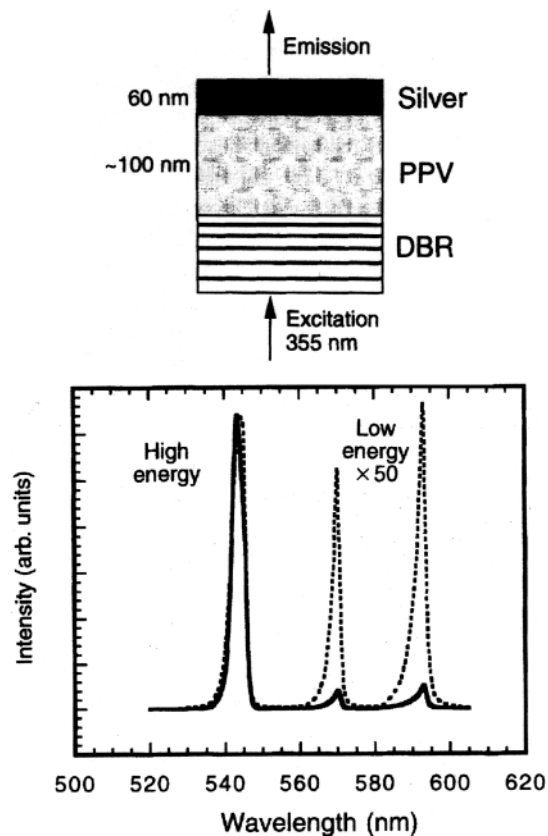


Figure 9. (a) Schematic structure of planar microcavity laser based on PPV and (b) emission spectra when operating below (dotted line) and above (solid line) lasing threshold, showing laser light preferentially stimulated into only one of the resonant modes. Reprinted with permission from Macmillan Publishers Ltd: *Nature*, vol. 382, N. Tessler, G. J. Denton, and R. H. Friend, "Lasing from conjugated polymer microcavities", pp 695–697, copyright 1996.

density $\sim 200 \mu\text{J cm}^{-2}$), the emission was stimulated preferentially into only one spectral mode, near the peak of the gain of PPV (see Figure 9). This mode ultimately dominated the emission spectrum of the laser.

It is remarkable to note that the gain medium in this laser was only 100 nm in length along the resonator axis, showing the enormous gain available from conjugated polymers. If one assumes a round-trip loss of $\beta \approx 30\%$, the gain coefficient $g \approx 20\,000 \text{ cm}^{-1}$! It should also be noted, however that exceptionally thin microcavities can in principle exhibit thresholdless lasing.⁹⁶ A microcavity of half a wavelength in thickness can substantially modify the spatial distribution of spontaneous emission from a material placed within the cavity via interference effects. In the photon mode picture, we can think of this as reducing the total number of allowed photonic modes for spontaneous emission. If the number of photon modes is reduced, then more of the spontaneous emission is channeled into the lasing mode, which effectively increases the emission cross section and ultimately reduces the pumping rate required to achieve lasing threshold. Experimentally, however, ideal microcavities are difficult to fabricate and usually have many in-plane modes, giving a reduced but nonzero threshold. Granlund et al. have shown that a conjugated polymer microcavity can increase the coupling of spontaneous emission into the lasing mode by 2 orders of magnitude compared with a conventional polymer waveguide.⁹⁷ The increased coupling will

therefore partly explain the apparently enormous gain coefficient.

Following on from this first study of planar microcavity lasers, there have been a number of other studies of OSL microcavities, based on a range of materials.^{22,29,36,78,97–106} Both transform-limited linewidths⁹⁸ and highly polarized emission^{97,101} have been demonstrated. Symmetric structures with low-loss dielectric Bragg reflecting mirrors on both sides of the polymer film have also been studied. Such structures have been demonstrated by sandwiching together two polymer-coated mirrors,^{97,101,103–105} and more recently, structures in which the top dielectric Bragg mirror has been directly deposited onto the organic semiconductor have been demonstrated.¹⁰⁴ Such lasing structures are comparable to the vertical cavity surface emitting lasers¹⁰⁷ (VCSELs) that have been widely studied in inorganic semiconductors and have the attractive features of low oscillation threshold combined with a low-divergence, surface-emitted output. A variant on such lasers are vertical external cavity surface emitting lasers¹⁰⁸ (VECSELs) in which one of the mirrors is in direct contact with the gain material and the second curved "external" mirror is spaced a small distance from the gain medium.^{109–111} Such structures have definitively shown the impact of the resonator on the polymer laser emission and hence clearly confirmed the resonant nature of the lasing.¹⁰⁹

3.3. Fabry–Perot Waveguide Lasers

An alternative configuration of the Fabry–Perot-type resonator is to arrange the resonator axis parallel to the plane of the film, rather than perpendicular as in the microcavity. In such a structure, the light is waveguided in the high refractive index organic film via total internal reflection at the semiconductor–air and semiconductor–substrate interfaces. To form mirrors at either end of the waveguide one must cleave the structure to create a flat end to the waveguide. This is the most common, low-cost configuration for inorganic semiconductor lasers, in which the semiconductor crystal may be readily cleaved to form very flat facets of typically 30% reflectivity, due to the very high refractive index of the semiconductor. For organic semiconductors, this is rather less attractive because the refractive index of organics is typically only half that of their inorganic counterparts. In practice, it is rather difficult to form good quality edges with polymer films, though such laser cavities have been successfully demonstrated in both evaporated films^{76,78,94} and molecular crystals.^{112–116} Kozlov et al. demonstrated such a laser based on Alq_3 doped with DCM2 with a 1 mm long cavity, many orders of magnitude longer than the microcavities described above and as a consequence requiring a much lower excitation density ($1 \mu\text{J cm}^{-2}$) to attain threshold.⁷⁶ The output emission was very efficient but highly divergent perpendicular to the plane of the film due to the emission coming from a subwavelength aperture at the end of the waveguide. An alternative mirror configuration is to use distributed Bragg reflector (DBR) gratings in place of the end facets. Such grating reflectors, which are discussed in more detail in section 3.6, both avoid the need for end facets and allow higher reflectivities or surface emission. Berggren et al. demonstrated a DBR laser in a comparable small molecule blend to Forrest's work and

measured a similar threshold density.⁷⁵ Fabry–Perot polymer fiber lasers have also been demonstrated using conjugated polymer and small molecule emitters.^{117–119}

3.4. Microring and Microsphere Resonators

One of the key advantages of organic semiconductors is the simple solution processing that permits some very novel fabrication methods that are impossible with inorganic semiconductors. Such novel processing has allowed the demonstration of other less conventional microresonator structures in polymer lasers, notably microlasers with annular or even spherical resonator structures. One example of this is the polymer microring laser,^{109,120–125} which consists (as shown in Figure 8c) of a thin polymer waveguide deposited around a dielectric or metallic core. These structures can be readily fabricated from solution simply by dipping the core, which may be a silica optical fiber or metal wire, into a concentrated solution of the polymer. On withdrawal of the fiber from the solution, an annular droplet surrounding the core dries to deposit a thin polymeric film. An alternative approach is to deposit a polymer on the inner surface of a microcapillary, which has the advantage of encapsulating the organic film.¹²⁶

Such films form a type of ring cavity broadly analogous to that shown in Figure 7b. Reflection of the light beam around these structures, however, works by total internal reflection of the light at the interfaces between the polymer and surrounding media. These lasers are rather larger in dimension than the planar microcavities, in that the diameter, D , of the cores are typically tens to hundreds of micrometers. The round trip path of the resonator is approximately equal to πD , and hence light travels through a much longer path of the gain medium in a round trip. Assuming that the round-trip losses are not substantially greater than in the case of the planar microcavity, this means that a much lower excitation density ($\sim 1 \mu\text{J cm}^{-2}$)^{120,123} is required in order to achieve sufficient gain to reach lasing threshold. Lasers with very low threshold pulse energies of 100 pJ have also been reported.¹²¹ Typically these lasers are pumped on one side of the ring, though axial pumping (in which the pump light is sent down the core of the ring) can lead to reduced threshold densities due to a more uniformly pumped structure.¹²⁷ These structures can also be configured as light-emitting diodes and so have the possibility of electrical excitation for lasers by using gold wire as the core and depositing a partially transmitting outer contact.¹²⁸ However, lasing has only been achieved by optical pumping (see section 5.1).

The longer round-trip distance, however, means that there are commonly many more longitudinal modes supported by the cavity, so these lasers tend to oscillate on many closely spaced wavelengths. The feedback mechanism can also be rather complicated,^{120,124} with a combination of whispering-gallery modes, in which total internal reflection around the ring can form a closed-loop optical path, plus other waveguide modes, in which light is trapped in the polymer film by total internal reflection at both polymer–air and polymer–core interfaces. Each mechanism supports a distinct set of resonant frequencies. These are superimposed to give complicated clusters of closely spaced modes within the polymer gain bandwidth (Figure 10). For sufficiently small diameters, $< 10 \mu\text{m}$, these clusters can be engineered to give single-frequency lasing. In addition to the often complicated spectral output, these resonators are distinctive in that they do not emit a

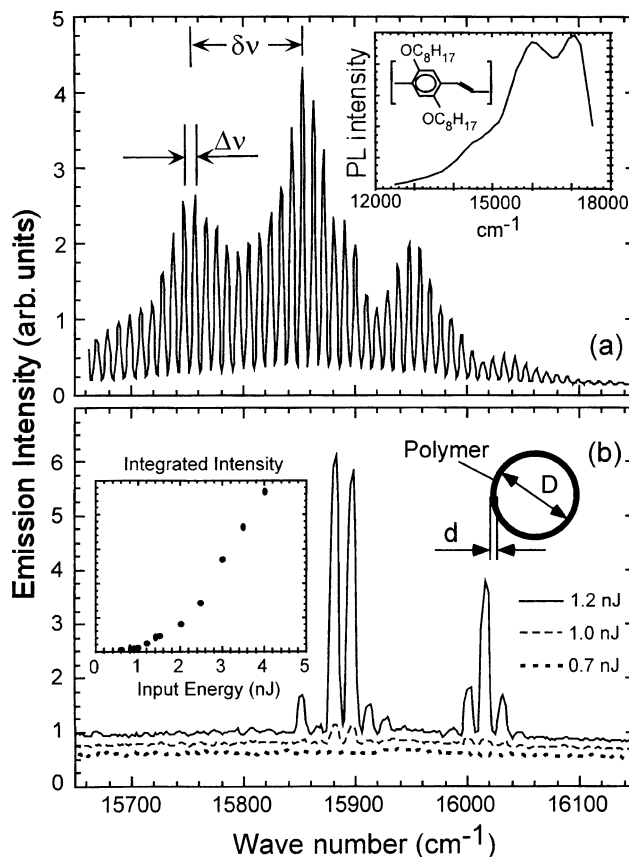


Figure 10. Typical lasing spectra from conjugated polymer microring lasers, showing the complicated clusters of closely spaced modes arising from the superposition of waveguide and whispering-gallery mode resonances. Insets show the emission spectrum and chemical structure of the polymer used, a schematic of the resonator structure, and the integrated power characteristics of the lasers. Reprinted figure with permission from S. V. Frolov, M. Shkunov, Z. V. Vardeny, and K. Yoshino, *Physical Review B*, vol. 56, pp R4363–R4366, 1997 (<http://link.aps.org/abstract/PRB/v56/p4363>). Copyright 1997 by the American Physical Society.

well-defined directional output beam; instead light is emitted uniformly in all radial directions. While this may generally be considered an unappealing feature, such an unusual output pattern may have some potential for sensing applications, as will be discussed in section 4.

Related geometries to the microring resonator are the microdisk^{129–131} and microsphere¹³² cavities. The microdisk is formed by lithographically patterning, then etching, an organic semiconductor film to form circular disks of ~ 3 – $20 \mu\text{m}$ diameter.^{75,133} These disk lasers support whispering gallery modes similar to those in the microrings. The microspheres are fabricated from microdisks by melting and resolidifying the semiconductor on a lyophobic surface, to form small solid droplets of organic semiconductor. Such beads can also support a whispering-gallery resonance of potentially much higher quality than the ring.¹³²

3.5. Macroscopic Laser Resonators

There have been several studies of lasers based on conjugated polymers in liquid or solid solutions. These are usually configured as conventional dye lasers, with resonators of a few centimetres in length. In these lasers the conjugated polymer is diluted (at typically a few parts per thousand concentration by weight) in a solvent^{10,13,23,55,81,134–136} or passive polymer host.^{53,137,138} Typical resonators either

comprise a pair of mirrors around a cuvette or polymer block, or include a diffraction grating in place of one mirror, in either a Littrow or Hänsch cavity configuration (the diffraction grating may replace the mirror by orienting it such that the first-order diffracted light is retroreflected back into the cavity. By rotating the diffraction grating, one may thereby tune the lasing wavelength). Indeed the first example of a conjugated polymer laser, reported by Moses in 1992, was of this type.¹⁰ A 10 mm cuvette of poly(2-methoxy-5-(2'-ethylhexyloxy)-1,4-phenylene vinylene) (MEH-PPV), at a concentration of 0.21 mg/mL in chloroform, was sandwiched between a pair of parallel planar mirrors to form the resonator. One mirror was highly reflecting, and the other a 3% output coupler for the lasing wavelength of 600 nm. This laser exhibited a threshold of 450 μJ and an output pulse energy of 2.6 μJ at 500 μJ pumping rate. Such macroscopic lasers tend to operate with much higher energies than the microcavity structures, commonly with thresholds of tens to hundreds of microjoules and output pulse energies of a few microjoules up to ~ 0.7 mJ in the case of the work of Brouwer et al.⁸¹ While these lasers are usually in a non-semiconducting host, (an exception was the work of Kumar et al., who blended a PPV derivative in PVK to produce a semiconducting slab laser of centimeter dimensions),¹³⁷ they provide a useful comparison to the performance of conventional dye lasers. Such comparisons have shown that conjugated polymers perform as well as common rhodamine and coumarin laser dyes,^{10,81} while offering the advantages discussed in section 2.4.

3.6. Diffractive Resonators

A final key class of resonator for organic semiconductor lasers are diffractive structures. These resonators do not use either mirrors or total internal reflection for feedback, but instead use periodic, wavelength-scale microstructures that diffract, or Bragg-scatter the light (Figure 8e,f). These periodic structures can be readily incorporated into planar organic semiconductor waveguides and avoid the need for good-quality end facets to provide the feedback.

By imposing a periodic surface corrugation on the organic semiconductor film, one may create a structure that will reflect propagating waveguide modes without needing to form end facets. There have been many different diffractive structures explored for organic semiconductor lasers, including simple diffraction gratings that form so-called distributed feedback (DFB) lasers, two- and three-dimensional photonic crystal structures, and concentric circular gratings that provide a radial feedback about a particular point. There have also been lasers with aperiodic feedback structures based on high-rotational-symmetry photonic quasi-crystals, or even with completely random scattering centers that may provide closed-loop feedback in the films. Distributed feedback lasers have proved particularly successful and are discussed in more detail in the following subsections

Figure 11 shows a typical structure of a polymer DFB laser with diffractive feedback along one axis in the plane of the waveguide. The laser consists of a thin organic semiconductor film deposited on top of a corrugated fused silica substrate. Light propagating in a waveguide mode of the high-index organic film is scattered by the periodic corrugations. The scattered light from each corrugation combines coherently to create a "Bragg-scattered" wave propagating in some new direction. The angle through which the light is Bragg-scattered, or diffracted, is highly wavelength-

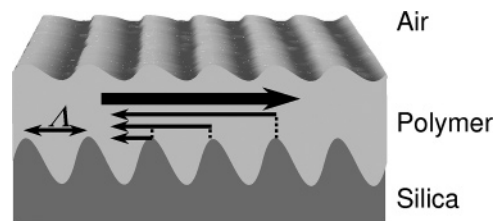


Figure 11. Schematic structure of a polymer DFB laser with corrugations of period Λ . Light of wavelength $\lambda = 2n_{\text{eff}}\Lambda$ propagating from left to right is scattered from the periodic structure to create a diffracted wave propagating in the counterpropagating waveguide mode.

dependent, so one finds that different wavelengths are diffracted into different directions.

For a given period of the corrugation, there is a particular set of wavelengths that will be diffracted from a propagating mode of the waveguide into the counterpropagating waveguide mode. This situation will arise when the Bragg condition is satisfied:

$$m\lambda = 2n_{\text{eff}}\Lambda \quad (6)$$

Here, λ is the wavelength of the light, Λ is the period of the structure, and m is an integer that represents the order of the diffraction. n_{eff} is the so-called effective refractive index of the waveguide; this is a geometrical average of the refractive indices of the three layers of the waveguide and may be calculated through a solution of the Helmholtz wave equation for a planar multilayer structure. For first-order diffraction therefore the wavelength of the reflected light will equal twice $n_{\text{eff}}\Lambda$. For the case of $m = 2$, the reflected wavelength is equal to $n_{\text{eff}}\Lambda$, but now light is also diffracted out of the surface of the film perpendicular to the plane of the waveguide. Such second-order structures can therefore provide a surface-emitted output coupling of the laser light via first-order diffraction while providing in-plane feedback via second-order diffraction.

The full theory of DFB lasers is somewhat more complicated than this simple diffractive picture, since the wavelength that exactly satisfies the Bragg condition cannot propagate in the film. This leads to what is known as a photonic stopband, centered on the Bragg wavelength, for light propagating in a direction perpendicular to the grating grooves. (In an extreme example of such a structure, in which there is a two- or three-dimensional grating and very strong feedback due to a large refractive index difference between the component materials, the photonic stopband can become a full photonic band gap, for which a range of wavelengths are forbidden from propagating in any direction. The photonic band gap is analogous to the electronic band gap caused by the Bragg scattering of the electron wavefunction in an atomic crystal.) This behavior is described by the coupled mode theory of Kogelnik and Shank¹³⁹ that predicts that the DFB laser will normally oscillate on a pair of wavelengths, one at either edge of this photonic stopband. The spacing between these wavelengths is determined by the strength of the diffractive coupling of the counterpropagating waves. Thus this diffractive structure has an advantage over the Fabry-Perot lasers in that it provides both a long resonator length in which the optical field can interact with the gain medium (and hence give a low oscillation threshold), and strong spectral selection of the resonant light. DFB lasers based on inorganic semiconductors are commonly used in telecommunication applications, taking advantage of the

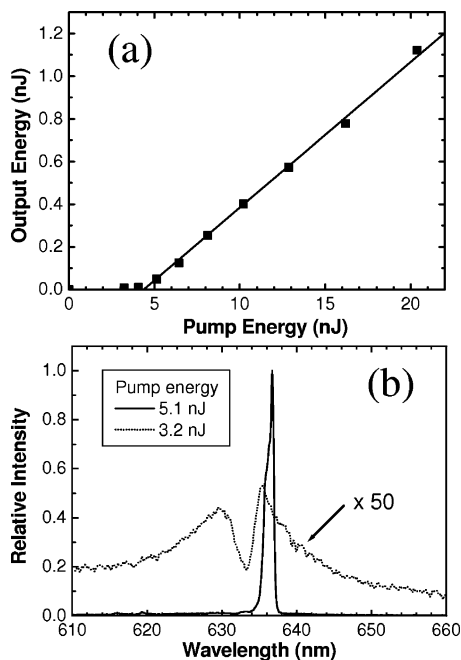


Figure 12. (a) Energy characteristic of square-array DFB laser and (b) normalized emission spectra above and below lasing threshold, showing lasing at the edge of the photonic stopband. Reprinted with permission from *Applied Physics Letters*, vol. 82, G. A. Turnbull, P. Andrew, W. L. Barnes, and I. D. W. Samuel, "Operating characteristics of a semiconducting polymer laser pumped by a microchip laser", pp 313–315. Copyright 2003 American Institute of Physics.

stable spectral output for multiplexing many wavelength channels together.

Figure 12 shows typical spectral and power characteristics of a two-dimensional polymer DFB laser based on MEH-PPV with a second-order grating.¹⁴⁰ Below threshold, the fluorescence spectrum emitted perpendicular to the substrate is characterized by a pair of Bragg-scattered peaks, between which there is a photonic stopband. The laser has a threshold of 4 nJ, above which the power climbs linearly with excitation density, with a power slope efficiency of 6.8%. A narrow lasing peak, much less than 1 nm in linewidth, then dominates the surface-emitted output spectrum that appears at the edge of the photonic stopband.

3.6.1. One-Dimensional Distributed Feedback Resonators

DFB lasers with one-dimensional feedback have been demonstrated using many different organic semiconductors, including derivatives of poly(phenylene vinylene)s,^{26,52,77,141–144} polyfluorenes,^{33,49,82,145–148} and ladder-type poly(*para*-phenylene)s.^{149–153} They have also been studied in a number of small molecule systems,^{44,50,150,154–163} which have either been vacuum-evaporated or solution-deposited, including spiro materials^{44,50,164,165} and energy transfer blends commonly based on Alq₃ hosts doped with laser dyes.^{150,154,156,159} Polymeric energy transfer blends have also received growing interest^{49,166,167} and have facilitated some remarkably low lasing thresholds.

DFB lasers can exhibit very low thresholds, particularly for first-order feedback where output coupling losses are low. In DFB lasers of several millimeters length, side-pumped threshold densities as low as 200 nJ cm⁻² have been reported for small molecule blends¹⁶³ and 40 nJ cm⁻² for conjugated polymers.¹⁶⁸ In shorter DFB lasers (~100 μm long), threshold pump pulse energies of a few nanojoules are common, and

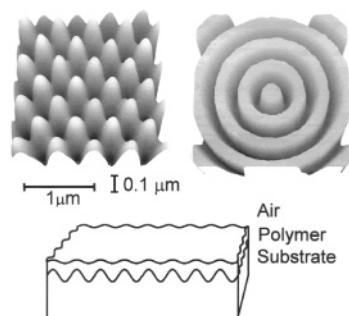


Figure 13. Atomic force microscope images of square lattice and CDFB surface gratings on SiO₂ substrates. The CDFB grating is written using electron beam lithography into a resist layer before being transferred into the SiO₂ using reactive ion etching. The sinusoidal profile of the square lattice grating originates from the double holographic exposure of interfering laser beams written into a photoresist layer, which is subsequently etched into the SiO₂ substrate. Both gratings are used for surface-emitting DFB lasers with feedback around 630 nm; a schematic of the waveguide laser structure is also shown, including the active polymer film.

they can be below 200 pJ for first-order structures.¹⁴⁸ There have been relatively few measurements of absolute slope efficiency from these lasers, though slope efficiencies of a few percent appear to be typical from the surface-emitting structures.¹⁴⁵ By changing either the period of the grating or the thickness of the waveguide (and hence its effective refractive index), one may readily tune the lasing wavelength over a range of typically 20–50 nm.^{33,49,50,52,146,154,156,169–171} Indeed a tuning range as large as 115 nm has thus been demonstrated in an Alq₃/DCM2 blend.¹⁷²

3.6.2. Two-Dimensional Distributed Feedback Resonators

In addition to the basic DFB laser, there has been growing interest in recent years in more complicated diffractive resonators that may apply a 2D feedback in the plane of an organic semiconductor film. These structures commonly form a 2D photonic crystal with either square,^{31,32,54,140,145,152,171,173–175} hexagonal,^{153,155,176} or honeycomb lattices,¹⁵⁵ though they also include other novel structures such as concentric circular DFB (CDFB) resonators,^{177–182} aperiodic quasi-crystals,¹⁸³ and even random-scattering structures.^{133,184–188} Figure 13 shows atomic force microscope images of square-array and CDFB feedback gratings used in polymer lasers.

In such resonators, feedback may be applied in several directions in the plane of the film, characteristic of the symmetry of the 2D pattern. The exact nature of the feedback depends upon both the symmetry of the grating and the relative values of the lattice period and the wavelength that experiences gain. For a square lattice, for example, feedback is applied in two orthogonal directions in the plane of the film. These are usually parallel to the two fundamental crystal planes,^{31,32,54,140,145,171,173,174} although feedback may also be applied along the diagonal symmetries for an appropriate wavelength of light.¹⁷⁵ For a hexagonal lattice, there are more symmetry axes; feedback in such a structure based on Alq₃/DCM has been comprehensively characterized by Notomi et al.¹⁷⁶

The case of CDFB lasers is subtly different, in that feedback can be applied in all directions in the plane about a single unique point that is located at the center of the grating.^{177–182} Light emitted at this central point will experience a photonic stopband for all in-plane directions of propagation, resulting in a photonic band gap for a small

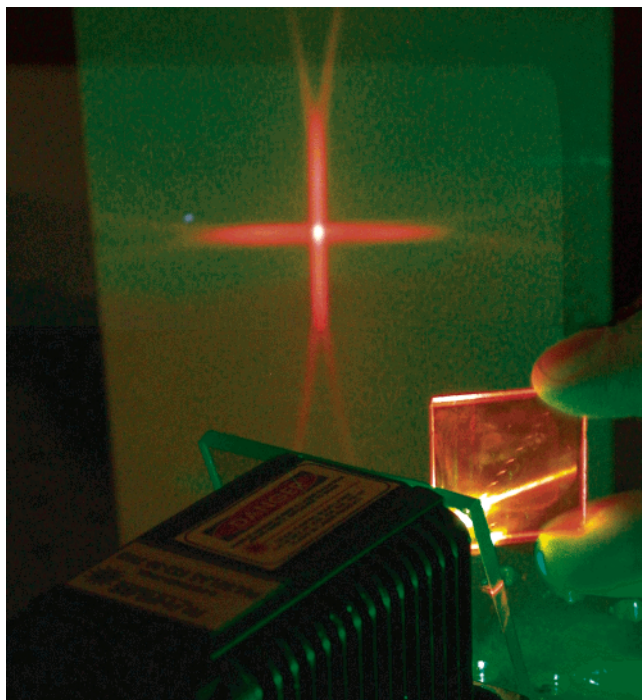


Figure 14. Square-array polymer DFB laser (based on MEH–PPV) pumped by a microchip laser. The surface-emission pattern is typical for a DFB structure consisting of two perpendicular gratings when pumped far above threshold; at lower pumping powers, only the bright central annular beam is emitted. Reprinted from *Materials Today*, vol. 7, I. D. W. Samuel and G. A. Turnbull, “Polymer lasers: recent advances”, pp 28–35, Copyright 2004, with permission from Elsevier.

range of frequencies.¹⁷⁸ Unusually, this can happen for a structure with very low index contrast. The lasing mode in a CDFB laser is thus very strongly confined to the center of the laser.¹⁸² CDFB resonators have also formed the basis of a two-photon pumped polymer laser. The feedback in quasi-crystal resonators, such as those based on a Penrose lattice, is rather more complicated but can support a range of laser modes. Notomi et al. showed that the quasi-crystal lasing is a result of well-defined extended modes, coherent over a length $>100\times$ the quasi-lattice constant.¹⁸³

The motivation for studying such 2D DFB structures is more than just scientific curiosity, because these have been shown in a number of studies to exhibit improved operation in OSLs. For while the 2D lasers also combine excellent spectral selection with a reasonably long cavity length, they can exhibit improved output beam quality, lower threshold, and higher output efficiencies than their 1D counterparts. Riechel³¹ and Heliotis¹⁴⁵ have made direct comparisons of 1D and 2D feedback in polymer lasers and have observed a dramatic improvement in beam quality. For a surface-emitting 1D DFB laser, the output beam is emitted as a divergent stripe, parallel to the orientation of the grating grooves. In the 2D structure, at modest excitation densities, the output beam has a divergence of typically only a few milliradians in any direction and is close to being diffraction limited. Such output beams were observed by Turnbull et al. to be annular and have an unusual azimuthal polarization state.¹⁴⁰ At higher pumping powers, the emission forms a cross shape, mimicking the symmetry of the grating, as illustrated in Figure 14. The 2D structure has been shown to reduce the oscillation threshold by a factor of 20, to 0.8

nJ for a polyfluorene gain medium, with a corresponding 3.5 times increase in the output slope efficiency to 7.8%.¹⁴⁵

3.6.3. Three-Dimensional Distributed Feedback Resonators

Three-dimensional photonic crystal resonators have been demonstrated by back-filling synthetic opals with conjugated polymers and organic dyes in solution and solid state. Lasing and ASE have been reported,¹⁸⁹ as well as the impact of the resonances on other optical transitions.¹⁹⁰ Defect modes arising from imperfections in the synthetic opals have been found to be significant in these structures.

Another 3D feedback structure of note is random lasers^{133,184–188,191–193} that, for example, contain TiO₂ spheres blended with a conjugated polymer or inhomogeneities in the organic semiconductor film itself.^{184–188,192,193} These can support irregular closed-loop paths around which certain wavelengths may be amplified. The lasing spectra of such scattering structures are random as the name would suggest, and these lasers tend to oscillate on a cluster of frequencies, the precise values of which vary across the film. Polson et al. have made some nice studies of the spectral properties of these unusual “resonators” and have shown that they exhibit a universal property in that the underlying random resonators responsible for the laser emission are almost identical to each other, which results from the large optical mean free path, $\sim 10\lambda$.¹⁸⁵

3.6.4. Photonic Design of Diffractive Organic Semiconductor Lasers

In order to harness the advantages of these more complex resonators, it is important that one can understand the interaction between the wavelength-scale periodic structure and light that is emitted within it. Consequently there have been a number of studies aiming to understand the emission behavior of organic semiconductor DFB lasers. Commonly this has been achieved through an analysis of the photonic band structure, or photonic dispersion, of the devices. The photonic band structure (illustrated for a hexagonal lattice OSL in Figure 15) is strongly analogous to the electronic band structure of a real crystal of atoms and shows the relation between the energies of the particle (the photon) and its wavevector or momentum in a given direction within the lattice.¹⁹⁴ Such a picture reveals bands of photon energies separated by gaps (or at least stopbands for certain propagation directions) that can reveal information about the group velocity of light propagating through the crystal related to the gradient of the dispersion diagram and explain the discrete directions of propagation that are possible for particular photon energies. The location of these photonic stopbands correspond to solutions of the Bragg equation for given propagation directions, while knowledge of the Brillouin zone can help predict the emission directions of the output laser beams. Calculation of these photonic dispersions may be complicated,¹⁹⁴ but this approach may be used to successfully predict the lasing wavelengths from knowledge of the geometry and dimensions of the feedback structure and refractive indices of the component layers of the waveguide. Several groups have attributed lasing wavelengths in their devices to particular photonic stopbands in the photonic dispersion and hence to particular feedback modes within the organic photonic crystal.^{32,141,143,152,153,169,175,176,195} Meier et al. have shown the correspondence of output beams, including so-called Kikuchi

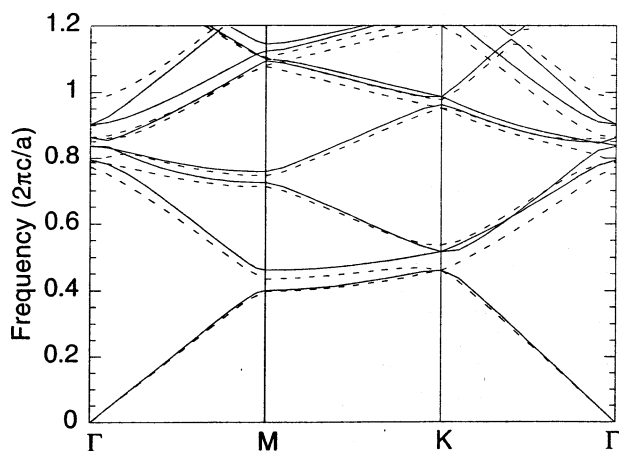


Figure 15. Photonic band dispersion plot of photon energy versus in-plane wavevector for a 2D triangular lattice of air holes in a dielectric of refractive index 1.5. The lattice constant is a ; Γ , M , and K correspond to the main symmetry directions in the triangular lattice. Solid lines represent transverse electric waveguide modes, and dashed lines represent transverse magnetic modes. DFB lasing can typically occur at the point at which the gradient of the dispersion curve goes to zero. Reprinted from *Applied Physics A*, vol. 69, (1999), pp 111–114, “Lasing mechanism in two-dimensional photonic crystal lasers”, A. Mekis, M. Meier, A. Dodabalapur, R. E. Slusher, and J. D. Joannopoulos, Figure 2, copyright 1999. With kind permission of Springer Science and Business Media.

lines, to the crystal symmetries of square, hexagonal, and honeycomb lattices,¹⁹⁵ while Riechel et al. have explained properties of the emission beam using the Laue formalism of diffraction from crystal structures.³¹

Turnbull et al. have taken a different approach of directly measuring the photonic dispersion of polymer DFB lasers, using a combination of angle-dependent transmission and photoluminescence, illustrated in Figure 16.^{32,141} Such a combination of measurements can provide information on the feedback of counterpropagating waveguide modes and their output coupling to free space. The experimental observations on a particular laser structure have the advantage that they probe the optical properties of the real structure, rather than some theoretical approximation to it. Such an approach has provided specific insight to the spectral properties of DFB lasers, for example, by relating single-frequency band-edge oscillation of surface-emitting DFB lasers to the very different output-coupling efficiencies of the two band edges.¹⁴¹

While the photonic crystal structure has a strong impact upon the coarse spatial and spectral properties of the laser output, other aspects of the diffraction grating can have a dramatic impact on the threshold of the device. To quantify their influence on threshold, the coupled wave formalism, mentioned above, is the most useful approach. It is well recognized that first-order DFB lasers are likely to have lower thresholds than second-order DFB lasers, since they have no coherent surface output coupling losses. However, other more subtle aspects of the grating structure can also have a substantial impact upon the threshold. For example, Barlow et al. have shown that the shape of the grating teeth can strongly affect the relative strengths of in-plane feedback and surface output coupling in a second-order DFB polymer laser and can lead to an order of magnitude change in threshold of the device.^{179,196} This effect has been observed experimentally in CDFB lasers.¹⁸¹

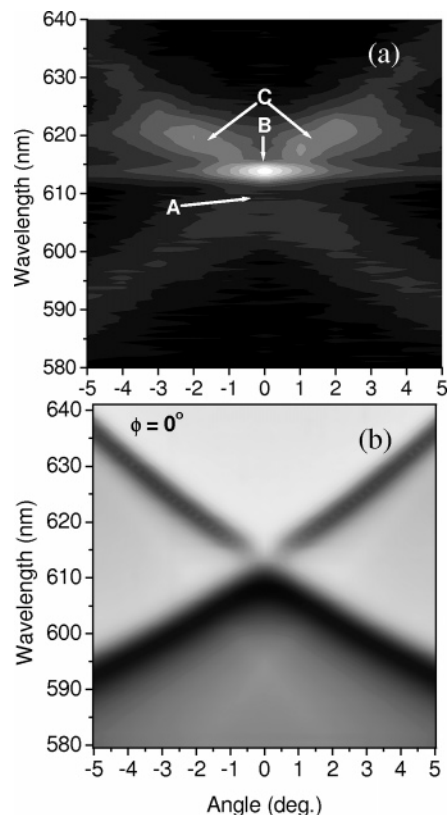


Figure 16. (a) Interpolated gray-scale images of experimentally measured angle-dependent laser emission from a surface-emitting polymer DFB laser; light regions represent the strongest emission (logarithmic contour interval). Labels A–C refer to (A) the dip in emission at the photonic band gap, (B) the intense laser emission, and (C) scattered ASE in the long wavelength emission band. (b) Angle-dependent transmission of light polarized parallel to the grating grooves, showing the coupling strength between the waveguide modes and free space beams; dark regions represent low transmission. Lasing occurs on the band edge with the lower output coupling losses to the surface-emitted beam. Reprinted from *Synthetic Metals*, vol. 127, G. A. Turnbull, P. Andrew, M. J. Jory, W. L. Barnes, and I. D. W. Samuel, “Emission characteristics and photonic band structure of microstructured polymer lasers”, pp 45–48, Copyright 2002 with permission from Elsevier.

The particular materials used within the grating structure can also strongly affect performance. While in most studies either a silica or inert polymer grating has been used, there have also been studies using metallic gratings,^{143,151} arrays of metal nanodiscs,¹⁷³ and titania and alumina gratings. Such materials can lead to much stronger confinement of the waveguide mode by exploiting large interfacial Fresnel reflections. However they may also introduce substantial losses,¹⁴³ thereby increasing thresholds, unless one carefully designs the optical structure to give a weak overlap of the resonant mode with the lossy (metallic) layers.^{151,173} The choice of the resonator materials can also permit unusual operating properties; for example, Berggren et al. tuned the wavelength of a DFB laser by bending the plastic substrate, thereby modifying the period of the grating,¹⁵⁴ while Suzuki tuned the grating period by squashing an elastomeric substrate.¹⁷⁰

There have also been reports of organic semiconductor DFB lasers in which no physical periodic structure is introduced.^{197–204} Instead, the thin film is photopumped with the interference pattern of two intersecting laser beams. Where the beams interfere constructively, there is a maximum in excitation density; where they interfere destructively

there is no excitation. The period of the resulting gain grating (and photo- and thermally induced index grating) depends on the intersection angle of the pump beams. This can be simply varied, giving another mechanism to tune the output wavelength.

3.7. Organic Semiconductor Laser Fabrication

A key advantage of organic semiconductors is their simple fabrication. Vacuum evaporation of amorphous organic films²⁰⁵ is much less demanding than epitaxial growth of inorganic crystals. Solution processing creates new possibilities for printing optoelectronic devices. A key example of the opportunities made by simple processing is the fabrication of microring resonators.¹²⁰ These can be made extremely simply by dip-coating a wire or optical fiber in a polymer solution; surface tension then shapes the low-loss annular resonators. It is also straightforward to deposit good optical quality thin films, multilayer heterostructures⁷⁶ and highly oriented birefringent films.^{56,101,206,207} These present a number of options for designing optical waveguides. Slab waveguides may subsequently be oxygen plasma etched to form various waveguide and resonator structures.

One complication in processing organic semiconductors is that only low temperatures may be used. This is particularly relevant for structures that combine organic and inorganic materials, such as microcavity lasers. Deposition of dielectric Bragg mirrors commonly requires processing above 200 °C in an oxygen-rich environment, which is likely to degrade the organic emitter. Recent progress in low-temperature deposition using thermal evaporation²⁰⁸ or electron-beam deposition¹⁰⁴ have addressed this and allowed low-threshold monolithic microcavity lasers to be made.

A final growing area of interest is in simple fabrication of diffractive OSLs. All such resonators require submicrometer periodic structures that are difficult to produce using conventional lab-based photolithography. Therefore the techniques used to define these structures have largely used holography or electron-beam lithography to write the patterns. The pattern is initially written in a photo- or electron-beam resist, which is chemically developed before being etched into a SiO₂ substrate. Holography has the advantage that large areas may be patterned. While confined to small areas (<1 mm²), electron beam lithography can allow the definition of complex structures, for example, CDFB gratings or multiperiod and photonic crystals. While such techniques are fine for the research laboratory, they remove one of the key advantages of any organic semiconductor device, simple processing.

Consequently, there have been a number of studies focused on the simple replication of these original structures, using processes that may potentially be scaled to volume production. One strategy is simply to pattern a passive polymer substrate, for example, by UV embossing,^{149,154,209} before depositing the active layer on top. With UV embossing, a hard master grating (made in SiO₂) is pressed into a passive organic film, which is then photopolymerized using UV light.¹⁵⁴ Alternatively a poly(dimethyl siloxane) (PDMS) elastomeric replica is made of the hard master structure and is then pressed into a liquid prepolymer during the UV irradiation.²¹⁰ The PDMS replica can itself be successfully used as the corrugated substrate for organic semiconductor lasers (OSLs).^{170,211} More recently, a growing number of studies have explored direct patterning of the active layer itself. These have used other soft lithographic techniques,

such as nanoimprint lithography (NIL)^{160,209,212–216} and micromolding.¹⁷⁴ NIL generally uses a combination of heat and pressure to imprint the surface structure of a master grating into a softened polymer film. As mentioned above, heating organic semiconductors above their glass transition temperatures (often in the range of 100–300 °C) can degrade the light emission; therefore such processes need to be carried out under vacuum or in an inert atmosphere.²¹⁷ Even then the polymers may crystallize on cooling, leading to significant diffuse scattering losses.²¹⁸ The requirement for high pressure can be relaxed by using an elastomeric master,^{213,216} which ensures conformal contact with the organic layer. Pisignano et al. have also demonstrated room-temperature NIL, which is more suitable for small molecule systems that exhibit poor thermoplastic properties.²¹⁴ An alternative room-temperature approach is to use solvents to enable the micromolding process. Two techniques that have been successfully applied to OSLs use solvent-assisted micromolding (SAMiM)¹⁷⁴ and liquid imprinting.²¹⁹ For SAMiM, an elastomeric master is inked with a solvent and placed in contact with a spin-coated film. The solvent redissolves the organic semiconductor film and allows it to conform to the mold. With liquid imprinting, a PDMS mold is placed in contact with a drop-cast solution of the polymer and allowed to dry. All of these techniques can be quick and simple and can readily reproduce feature sizes as small as 100 nm. A number of lasers with thresholds comparable to those using SiO₂ corrugated substrates have been demonstrated.

3.8. Resonator Conclusions

In conclusion, there have been a wide range of novel resonator structures employed for OSLs. This wide range is principally a testament to the flexible processing properties of organic semiconductors and includes some that are quite specific to the simple fabrication possible in these materials. There have also been a number of pieces of innovative work that have specifically employed the organic semiconductor gain medium as a convenient, processible microlaser gain medium with which to study new laser physics. As discussed in this section, emphasis in the past few years has strongly moved toward diffractive feedback structures, which can combine the advantages of low-threshold surface emission and good spectral selection. While the choice of gain medium will control the available spectral range within which the laser may work and can have some substantial impact upon the threshold and efficiency, as with any other laser the resonator in OSL provides substantial scope for engineering specific properties. Through choice of basic resonator structure and finer detail of the design, one may have substantial impact upon the oscillation threshold, output efficiency, emission beam pattern and finer aspects of the wavelength. The growing body of work in understanding and controlling these features is particularly relevant in the progress toward applications of these lasers. This is the topic of the next section of the review.

4. Toward Applications of Organic Semiconductor Lasers

While direct electrical pumping of OSLs remains one of the major outstanding challenges in the research of organic semiconductors (see section 5), optically pumped OSLs are in their own right attractive visible light sources. Typical oscillation thresholds for a range of resonator geometries are

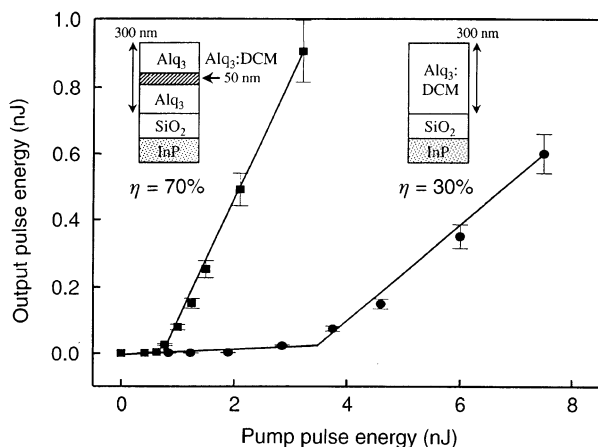


Figure 17. Power characteristic of 1 mm long slab waveguide (inset right) and double heterostructure (inset left) Fabry–Perot lasers based on Alq₃ doped with DCM laser dye. The double heterostructure device, which confines both the population inversion and optical mode in the DCM doped layer, exhibits a quantum slope efficiency of 70%. Reprinted with permission from Macmillan Publishers Ltd: *Nature*, vol. 389, V. G. Kozlov, V. Bulovic, P. E. Burroughs, and S. R. Forrest, “Laser action in organic semiconductor waveguide and double-heterostructure devices”, pp 362–364, copyright 1997.

sufficiently low that they may be very readily pumped by compact diode-pumped solid-state lasers, such as Nd³⁺ microchip lasers,^{33,140,156} and are even now within the range of direct excitation using GaN-based semiconductor diode lasers.^{49,220,221} Such compact systems combine high electrical wall-plug efficiencies with the broad tuning range of organic semiconductors. These compact, match-box-sized systems present an attractive potential platform for addressing a range of applications.

From an applications perspective, OSLs offer a range of generic attractive features. They can be simply processed and are inexpensive, may readily be integrated onto other technology platforms and offer broadly tuneable emission throughout the visible spectrum. Such features, and the emission wavelengths in particular, make OSLs particularly relevant to applications in spectroscopy and sensing but also to some areas of data communications and displays. In this section, we will discuss progress being made in such areas.

4.1. Progress in Laser Operating Characteristics

Any particular application will place specific requirements upon the operating properties of the laser source, including the power levels, pulse duration, repetition rate, spectral and spatial properties of the output beam, and operating lifetime of the device. So before addressing particular applications areas, it is useful first to review some of the progress in lasing operation in these areas.

4.1.1. Output Power

Quantitative measurements of the output power from OSLs are surprisingly sparse in the literature, with a large majority of papers concentrating only on the spectral properties of the output from the laser. Nevertheless, those papers that do characterize the output pulse energies have shown that OSLs can exhibit quite respectable differential slope efficiencies. The highest efficiency reported was for a DCM2 doped Alq₃ laser configured as a Fabry–Perot waveguide resonator.⁷⁶ This laser exhibited a 70% quantum slope efficiency (~35% power slope efficiency), with a maximum output pulse

energy of 0.9 nJ at a pump pulse energy of 3 nJ (see Figure 17). Second-order DFB lasers, meanwhile, have given surface-emitted power slope efficiencies of ~7% for MEH–PPV¹⁴⁰ and ~10% for poly(9,9-dioctylfluorene) (PFO)¹⁴⁵ with peak output energies of 1.1 nJ.

While nanojoule output energies have been typical in waveguide OSLs, one should note that the excitation volume of organic semiconductor is very small (~10⁻⁹ cm³). In larger external cavity OSLs, pulse energies of 0.7 mJ⁸¹ and slope efficiencies up to 15%¹³⁷ have been reported. Furthermore, while the energies appear to be quite modest, the short duration of the pulses means that peak powers at the Watt-level and above can readily be obtained, even in microlasers. As mentioned earlier, a distinctive feature of the power characteristics of OSLs is their insensitivity to temperature. Koslov et al., have shown that the threshold and slope efficiency of DCM-doped Alq₃ lasers is largely independent of temperature in the range of 0–140 °C.⁹⁴ Ramos-Ortiz et al., meanwhile, have observed a very weak temperature dependence on threshold in conjugated polymer microring lasers.¹²³ This feature is significantly different from the performance of inorganic semiconductor lasers, which need to be maintained at a tightly controlled temperature.²²²

4.1.2. Temporal Characteristics

While the temporal properties of liquid dye lasers may span a huge range of pulse durations from <10 fs to continuous-wave operation,⁹⁵ solid-state lasers are usually less adaptable. A common limitation to the continuous-wave operation of a solid-state organic laser is the accumulation of triplet excitons through intersystem crossing. These exhibit excited-state absorption losses, which can severely compete with the stimulated emission. OSLs therefore have been driven with pulsed excitation sources, typically in the 100 fs to 10 ns time regimes. Following excitation, the gain medium is given time to recover prior to the next excitation pulse arriving. Commonly the lasers are driven at repetition rates of between 10 Hz and 10 kHz, which is sufficiently low for any triplet populations (though possibly not thermal effects) to dissipate between pulses.

There have been a few studies of the temporal properties of the output pulses of OSLs. These include work by Van den Berg et al. who studied lasers based on a PPV-copolymer solution in a 25 mm long cavity. They observed trains of pulses spaced by half the cavity round-trip time of 200 ps.¹³⁶ They interpret the pulse train formation as resulting from multiple gain switching in a cavity whose lifetime is intermediate between the pump pulse duration and the gain medium lifetime. Studies of dynamics in microcavities have observed pulse trains on picosecond timescales.^{78,103} Pulsed outputs as short as 3.6 ps have been measured in a VECSEL structure based on a ladder-type poly(*para*-phenylene) (LPPP).¹¹⁰ Goossens et al. showed that gain-switched DFB lasers could generate subpicosecond pulses in a very simple laser structure (Figure 18)⁵⁴ and presented a simple model of the laser dynamics. Zavelani-Rossi et al. have studied the population kinetics of an operating DFB laser, using transient absorption with subpicosecond time resolution.²²³

Rabe et al. have demonstrated quasi-continuous wave lasing, with pulsed repetition rates of up to 5 MHz, in a polyfluorene derivative DFB laser. The prospect of true continuous-wave lasing would appear to be rather more challenging because of the long-lived triplet absorption and

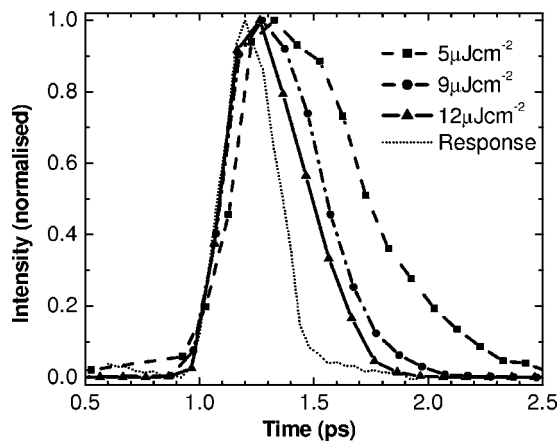


Figure 18. Output pulse dynamics from a surface-emitting polymer DFB laser pumped with 100 fs duration pulses. A minimum pulse duration of ~ 450 fs (full width at half-maximum) is measured using a femtosecond optical gating technique. Adapted from M. Goossens, Ph.D. thesis, University of St Andrews (2006).

photobleaching.²²⁴ However, Bornemann et al. have recently circumvented these in a continuous-wave pumped solid-state dye laser deposited on a rotating substrate.²²⁵ By rotating the laser very rapidly, one may mimic the circulating flow of a liquid dye laser that continuously refreshes the chromophores that are exposed to the excitation beam.²²⁶ While the output of this solid-state dye laser was rather noisy, it does provide an innovative approach that may be applicable to OSLs too.

4.1.3. Lifetime

A final important aspect of the power characteristics of OSLs relevant to their application is the lifetime stability of the device. All organic laser materials tend to degrade much more rapidly than inorganics due to photo-oxidation that quenches the emission. Again, there have been relatively few reports of the operating lifetime of OSLs, although Heliotis et al. have reported a lifetime of 2×10^7 pulses in a Dow Chemicals proprietary copolymer RedF.¹⁷¹ A LPPP VECSEL laser showed a lifetime of 3.6×10^7 pulses.¹¹⁰ Alq₃-DCM waveguide lasers meanwhile have exhibited 10^6 pulse lifetimes when pumping 100 times above threshold.⁷⁸ These values compare particularly well with solid-state dye lasers that typically exhibit lifetimes of 10^5 to 10^6 pulses.

4.1.4. Spectral Properties

In contrast to the data available on output powers, there is a very extensive body of work studying the spectral properties of OSLs. Broad-band spectral tuning of the output has been demonstrated in many different materials with tuning ranges of typically tens of nanometres in both conjugated polymers and small molecular systems. Tuning ranges in DFB lasers based on energy transfer blends can be particularly large: Heliotis et al. observed 75 nm of tuning in a polyfluorene blend.¹⁷¹ Schneider et al. have reported 72 nm of tuning in a blend of spiro molecules¹⁶⁴ and a 115 nm range in an Alq₃/DCM2 blend, as shown in Figure 19.¹⁷² Such huge tuning ranges are an order of magnitude larger than those typical in visible DFB lasers based on inorganic semiconductors.²²⁷ With appropriate material choice, one may generate OSL light throughout the visible spectrum. Recent progress has pushed lasing to 378 nm in the ultraviolet¹⁶⁵ and beyond 700 nm in the near-infrared.^{171,172} Generating longer wavelengths appears to be difficult in conjugated

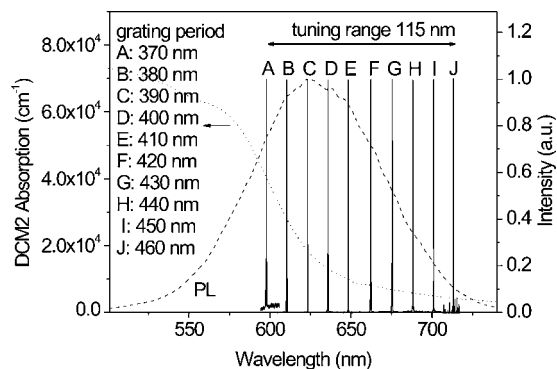


Figure 19. Lasing spectra for DFB lasers based on a single film of Alq₃ doped with the laser dye DCM2 for a range of feedback grating periods from 370 to 460 nm. The laser emission may be tuned through a range of 115 nm. The emission spectrum (dashed line) and absorption spectrum (dotted line) of DCM2 are also shown. Reprinted with permission from *Applied Physics Letters*, vol. 85, D. Schneider, T. Rabe, T. Reidl, T. Dobbertin, M. Kroger, E. Becker, H.-H. Johannes, W. Kowalsky, T. Weimann, J. Wang, and P. Hinze, "Ultrawide tuning range in doped organic solid-state lasers", pp 1886–1888. Copyright 2004, American Institute of Physics.

polymers because narrow band-gap polymers tend not to be very emissive. Alternatively, appropriate laser dyes can access the first telecoms window around 850 nm²²⁸ and even give electroluminescence out to 1200 nm.²¹⁵ Erbium-based organometallics²²⁹ or semiconductor nanocrystals^{230,231} may be promising dopants for light emission in the 1300 and 1550 nm telecommunication windows.

4.1.5. Beam Properties

The spatial properties of a laser beam are, as previously discussed, strongly dependent on the design of the resonator. By choosing suitable resonant structures, it should therefore be possible to generate high-quality, near-diffraction-limited laser beams. The strong birefringence of conjugated polymer films is helpful in this regard because it makes it straightforward to fabricate single waveguides that only support a single transverse mode, while still effectively absorbing the pump excitation wavelength. By working with waveguide structures that only support one transverse mode, the surface-emitted beam from second-order DFB lasers can be near diffraction limited and have low divergence.^{31,140} Where suitable end facets can be formed on organic waveguides, perhaps most easily achieved with organic crystals^{112–116} or evaporated small molecular films,^{76,78,94} there is a good prospect that these should emit good quality, though divergent, laser beams. While one may commonly want a very directional laser beam, the radial emission characteristic of microring and microsphere resonators may be interesting for some applications such as photodynamic therapy²³² or *in vivo* medical imaging.²³³ The recent demonstration of near-arbitrary control of output beam patterns and polarizations by Miyai et al.²³⁴ in inorganic photonic crystal lasers should be highly applicable to organic semiconductors. This may open up some new application areas.

4.2. Applications

Following a decade of research into the properties of OSLs themselves, a number of more applications-oriented projects are beginning to emerge. The output properties of OSLs described above show that these sources are already very good at generating wide ranges of wavelengths in short

optical pulses of modest pulse energies. This combination of characteristics suggests that they are well suited as spectroscopic light sources with potential for absorption measurements, fluorescence excitation, and even time-resolved studies. The spectral range covered is naturally suitable for spectroscopy of organic molecules including biological systems.

A first step in this direction was made by Schneider et al. using ultraviolet (UV) DFB lasers based on a novel spiro-linked material as the active organic layer.¹⁶⁵ These lasers generated light between 378 and 395 nm and were shown in a concept experiment to be suitable for exciting fluorescence in a number of dyes that are commonly used as biomarkers. Such UV excitation wavelengths may also be useful for *in vivo* cancer detection. The simple processing of organic materials makes organic semiconductors attractive light sources for integration into miniature spectroscopic systems. This has recently been demonstrated for solid-state dye lasers by Oki et al.,²³⁵ who measured the absorption spectrum of sodium vapor using an array of DFB dye lasers operating at a range of wavelengths. Balslev et al. meanwhile have demonstrated a complete on-chip integrated microfluidic dye laser with absorption cell and photodiodes.²³⁶ The advantages of organic semiconductors for efficiently converting pump light into the desired lasing wavelength, with improved operating lifetime and very low pump power requirements, make them very attractive candidates for similar spectroscopic studies. Furthermore, the prospect of being able to tune the emission wavelength by mechanically deforming the resonator¹⁷⁰ could be a very powerful feature for simple spectroscopic measurements.

Another rather different area for which organic semiconductors offer promise is the field of data communications. While global telecommunications are based on silica optical fibers carrying optical data pulses at around 1550 nm, short haul datacomms are increasingly using polymer optical fibers²³⁷ and planar lightwave circuits.²³⁸ Two areas in which this is becoming particularly important are the fiber to the home/workplace (FTTX) and in data transfer in automobiles. Each of these applications is very cost sensitive, and opto-coupling in broad-area graded-index polymer fibers is proving to be an attractive solution. Organic semiconductor gain media offer a potentially simple and compatible technology to act as optical amplifiers matched to the low-loss transmission windows in PMMA at 530, 570, and 650 nm. Conjugated polymers and dendrimers in solution have been shown to act as high-gain optical amplifiers,^{38,239,240} with gains of up to 44 dB/cm over a bandwidth of 50 THz.²³⁹ Amplifiers based on semiconducting polymers and dendrimers have been studied. Films, meanwhile, have exhibited gains at 660 nm of up to 18 dB in amplifier channel lengths of 300 μm (Figure 20).^{56,57} Organometallic erbium compounds doped in a passive polymer host have shown gains of 16.5 dB/cm at 1533 nm in a 20 mm long amplifier.^{229,241}

Organic semiconductors may also be useful for optical switching. Frolov et al. demonstrated ultrafast optical switching in poly(2,5-dioctyloxy-*p*-phenylene vinylene) (DOO-PPV) using a <10 ps control pulse at 610 nm that can dump the excited-state population back to the ground excited state, thereby reducing excited-state absorption at 1550 nm.²⁴² Virgili et al. have shown ultrafast gain switching in PFO using a femtosecond control pulse at 780 nm that can push the excited-state population into a higher excited state, thereby depleting stimulated emission over a 100 nm

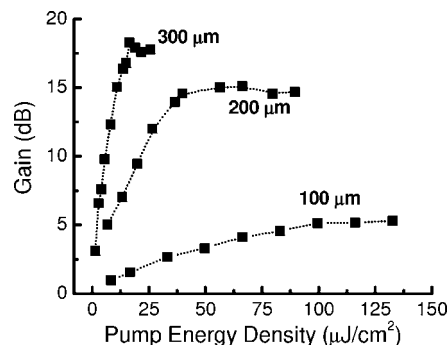


Figure 20. Gain characteristics for polyfluorene blend waveguide optical amplifiers. Peak gain is shown for a 100 fs probe pulse making a single pass through a range of amplifier channel lengths. Reprinted with permission from M. Goossens, G. Heliotis, G. A. Turnbull, A. Ruseckas, J. R. Lawrence, R. Xia, D. D. C. Bradley, and I. D. W. Samuel, "Semiconducting Polymer Optical Amplifiers", in *Proceeding of SPIE*, vol. 5937, *Organic Light-Emitting Materials and Devices IX*, p 593706. Copyright 2005, International Society for Optical Engineering.

bandwidth.²⁴³ Such devices could provide all-optical wavelength switching between near-infrared and visible datacomms channels.

A final applications area in which conjugated polymers show very exciting promise is in chemical sensing.²⁴⁴ One particular success is in detecting vapor of 2,4,6-trinitrotoluene (TNT) and 2,4-dinitrotoluene (DNT) using fluorescent-conjugated polymer thin films.^{245,246} The detection mechanism is based on the electron-deficient nitroaromatics reversibly binding to the electron-rich semiconducting polymer. This leads to an electron transfer that quenches the polymer's fluorescence. Since excitons on the polymer chain are mobile, one DNT molecule bound to the polymer may be able to quench any excitons initially generated some distance from the binding site. This increases the probability of quenching and provides a reversible mechanism for sensing the explosives. Rose et al. showed that this high sensitivity to explosives detection can be enhanced by more than 30 times when looking at the quenching of a laser operating close to threshold rather than spontaneous emission.¹⁶⁸ Their experiment was based on a PPV derivative configured as either a planar polymer film, a DFB structure, or a microring resonator. These devices were able to detect explosive vapors at the 5 ppb level, as illustrated in Figure 21. Conjugated polymer sensors based on similar reversible binding interactions have also been very successfully applied to detecting particular DNA sequences^{247–249} and various metal ions.^{250–252} These are based on fluorescence, and so there may be much wider opportunities for OSL sensors for detecting a range of systems at ultralow concentrations.

These examples illustrate the range of potential applications that OSLs may have, even when optically pumped. Such applications-based research is likely to grow in the future, and there are good prospects that OSLs will find niche-area applications, like the other more mature organic semiconductor technologies. The stability of these materials to photo-oxidation remains a significant issue, although this may be of only minor concern for the sensing and spectroscopic applications. Certainly, at present, one should regard OSLs as a disposable laser technology, though the low cost of the materials and simple fabrication suggest that this should not hinder developments toward market.

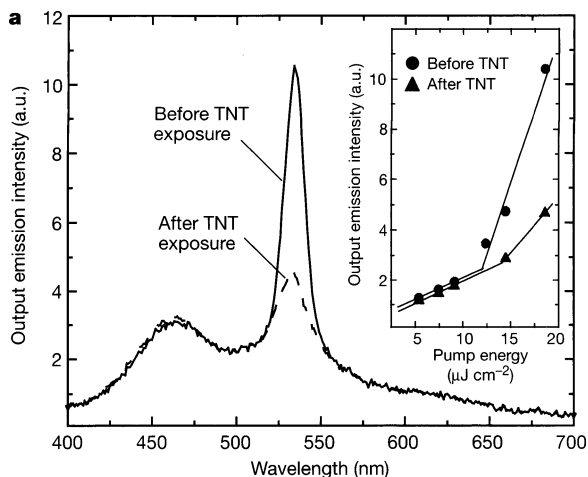


Figure 21. Response of the emission from a polymer microring laser to a 90 s exposure to 5 ppb concentration of TNT. A clear change in the stimulated emission peak is visible even in the absence of a change in the surrounding spontaneous emission spectrum. Inset shows the power characteristics before and after exposure. Reprinted with permission from Macmillan Publishers Ltd: *Nature*, vol. 434, A. Rose, Z. Zhu, C. F. Madigan, T. M. Swager, and V. Bulovic, "Sensitivity gains in chemosensing by lasing action in conjugated polymers", pp 876, copyright 2005.

5. Future Developments

5.1. Toward Electrical Pumping

All organic semiconductor lasers to date have been pumped optically. However, there have been two published claims of electrically pumped lasing.^{253,254} One was in tetracene crystals²⁵³ and was subsequently discredited and withdrawn.²⁵⁵ The other was in a structure with an indium metal contact containing aluminum tris(quinolate) (Alq₃) blended with Nile Blue.²⁵⁴ A narrow emission was reported at 410 nm. Because Alq₃ is a green emitter and Nile Blue is a red emitter, this emission cannot be attributed to the organic semiconductors present but may be due to indium, which has an atomic line at 410 nm. Further curious features of this report were that the device had linear current–voltage characteristics and that the alleged lasing started for an applied voltage of 0.27 V with a threshold current of 0.088 mA in a device of millimeter dimensions.

In this section, we will examine the challenges still to be overcome to achieve an electrically pumped laser. As discussed in other articles in this issue, organic LEDs have made tremendous progress in efficiency and durability over the past decade. While this is helpful for the development of OSLs, there are some important differences between lasers and LEDs. The first is that a laser must have a population inversion and so requires a much higher pumping rate than an LED. In this context the short (~1 ns) excited-state lifetime of organic semiconductors is demanding. The second difference is that lasers are very sensitive to losses (absorption) at the lasing wavelength. In contrast, light only needs to pass through 100 nm of material to leave an OLED. The third difference is that all OSLs have used fluorescent materials, whereas recent advances in high efficiency OLEDs have focused on phosphorescent materials. Because phosphorescence is a forbidden transition, the available gain would be orders of magnitude lower than that for singlets, which would mean, at the very least, that the laser would need to be orders of magnitude longer. Additionally, excited-state triplet absorption in these materials is likely to have

much higher transition cross sections than stimulated emission.

The three main issues to be considered relating to the feasibility of electrically pumped OSLs are the current densities required, the additional losses due to the contacts, and the additional losses due to the injected charges and triplet formation. A typical inorganic semiconductor diode laser operates at a current density of 1000 A cm⁻². In contrast a typical OLED in a display is operated at around 0.01 A cm⁻². It is not possible to pass 1000 A cm⁻² through current OLEDs continuously because they would overheat and be destroyed. This limitation relates to the low mobilities of organic semiconductors compared with their inorganic counterparts. For example, the hole mobility of the widely studied polymer poly(9,9-dioctylfluorene) is in the region of 4 × 10⁻⁴ cm²/(V s).²⁵⁶ We can consider the issue of current density for electrically pumped OSLs in two parts: what is the minimum current density required to reach threshold, and what is the maximum current density that can be passed through an OLED?

A lower limit on the current density required to reach threshold can be estimated using the threshold for optical pumping. The actual threshold will be much higher because of losses associated with contacts and carrier absorption, but it is a useful starting point, because even this lower limit is demanding. One example of such a calculation was by Kozlov et al. for a Fabry–Perot laser with a DCM-doped Alq₃ emissive layer in between Alq₃ layers.⁷⁸ The measured threshold pump energy density was 1 μJ cm⁻², corresponding to a photon density of 1.5 × 10¹² cm⁻². For a radiative lifetime of 5 ns, assuming a quarter of injected charges form singlet excitons would give a threshold current density of 200 A cm⁻² for 5 ns pulsed electrical excitation; 200 A cm⁻² would be far too high for continuous operation but can be achieved in pulsed operation (see below). The threshold can be reduced using a distributed feedback structure instead of a Fabry–Perot resonator, and for this situation, the threshold current density has been estimated at 80 A cm⁻²,¹⁶³ and a similar estimate has been made for a polymer DFB laser.¹⁸ Much higher current densities have been achieved in pulsed operation of very small structures with appropriate heat-sinking; 1000 A cm⁻² was achieved in light emitting polymers nearly a decade ago.²⁵⁷ Recently extremely high current densities of 12 000 A cm⁻²²⁵⁸ and 128 000 A cm⁻²²⁵⁹ have been reported in thin films of copper phthalocyanine. Although this material is not suitable for lasing, it nevertheless shows that organic semiconductors can sustain high current densities. Hence if there were no additional losses for electrical excitation, pulsed electrical pumping of an OSL would be feasible using current materials and device structures.

Unfortunately, there are additional losses associated with electrical pumping. One source of these is the contacts. In low-threshold OSLs, the resonator is in the plane of the film allowing long interaction lengths with the gain medium. This also means that there are long interaction lengths with the contacts, which absorb light. It is possible to achieve optically pumped lasing in the presence of a metal contact, but the threshold is greatly increased.¹⁴³ The effect of such a contact can be reduced by careful optical design so that the electric field profile of the waveguided mode has little overlap with the contacts and so suffers little absorption. This has been achieved for both small molecule^{163,260} and polymer lasers^{151,261} (see Figure 22), although in each case thin ITO

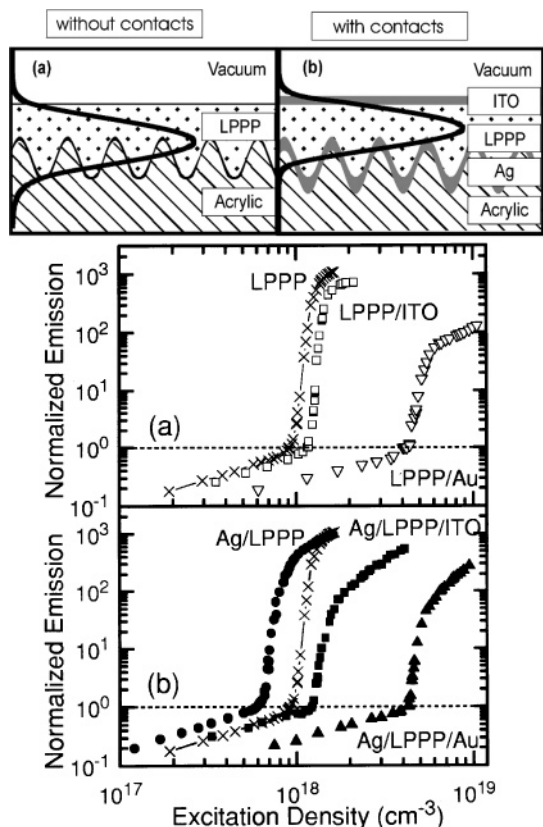


Figure 22. (a) Schematic of waveguide structure of a ladder-type poly(*para*-phenylene) DFB laser with and without electrical contacts and (b) optically pumped power characteristics (plotted on a log–log graph) of DFB lasers with a range of top electrodes (upper panel) and with the addition of a silver bottom electrode (lower panel). Lasing threshold corresponds to the excitation density for which each dataset crosses the horizontal dotted line. Reprinted with permission from *Applied Physics Letters*, vol. 84, M. Reufer, S. Riechel, J. M. Lupton, J. Feldmann, U. Lemmer, D. Schneider, T. Benstem, T. Dobbertin, W. Kowalsky, A. Gombert, K. Forberich, V. Wittwer, U. Scherf, “Low-threshold polymeric distributed feedback lasers with metallic contacts”, pp 3262–3264. Copyright 2004, American Institute of Physics.

was used as one or both contacts. The ITO was thin to prevent much of the mode being in it, but this has the consequence that its resistivity would be higher than is desirable for electrical pumping, especially at the high current densities required. These studies show that there is some tradeoff between optical and electrical properties but suggest that it is likely to be possible to achieve an acceptable compromise. Alternatively, recent progress in developing light-emitting transistors may offer an attractive geometry in which the contacts could be substantially separated from the optical mode in the gain medium.^{262–267}

There is a further and more serious source of loss associated with electrical pumping. Optical excitation mainly leads to the formation of singlet excitons,⁶⁰ which are exactly the excited states required to give gain. Electrical excitation involves charge injection followed by capture of charges to form an exciton, which can be singlet or triplet. The injected charges are referred to as polarons and have associated absorption. Similarly the triplet excitons also have associated absorption. Furthermore the polarons and triplets are likely to be far more abundant than the singlets in the device, Tessler estimates 1000 times as many polarons as singlets for a material with a mobility of 10^{-4} cm²/(V s).¹⁵ The crucial

issue, however, is whether these species absorb at the lasing wavelength.

The absorption of polarons and triplets can be measured in suitably designed experiments following either optical^{84,86,125} or electrical excitation.¹⁶³ These measurements show that the polaron absorption is typically broad and covers a wide spectral range, creating a problem for lasing. It is conceivable that materials innovations, including blending, could help. There are a number of detailed and interesting studies of the effect of contact and polaron losses on organic laser design and suggestions for the best candidate structures and materials requirements.^{163,268–271}

All three main issues outlined above relate to the low mobility of organic semiconductors. The low mobility makes it hard to achieve high current densities. It also means that losses due to absorption of the contacts cannot simply be resolved by making the light-emitting layer much thicker so that the electric field of the guided mode has little overlap with the contacts. The high concentration of polarons is due to their low mobility. Hence higher mobility helps with each of these issues, so recent reports of a polyfluorene-based material with mobility of 10^{-2} cm²/(V s) are encouraging.¹⁴⁷ It is however, a challenging problem to achieve high mobility, simple processing, high photoluminescence efficiency, and efficient charge capture all at the same time. In fact, OLED materials development has evolved in a different direction toward amorphous materials because they are less prone to recrystallization and less susceptible to intermolecular interactions, which can quench luminescence.

5.2. Indirect Electrical Pumping

As just explained, direct electrical pumping of an organic semiconductor diode laser remains a very difficult problem that will require significant further innovations. It is a very attractive goal because it would give simple low-cost battery-powered lasers across the visible spectrum, as well as the possibility of large arrays of lasers. There are plausible ways of achieving this outcome without direct electrical pumping and the associated challenges outlined above. These approaches involve indirect electrical pumping, in which an efficient electrically driven light source is used to pump an OSL optically. In this approach, charges are not injected into the lasing medium, removing the problems of polaron absorption. In addition the compromises outlined above between electrical and optical design of the OSL are removed, because the OSL is optically pumped. As mentioned in the previous section, considerable progress has been made in reducing the size of pump lasers from the regenerative amplifier, covering a large optical table, originally used.¹¹ By improving optical design to reduce threshold, microchip lasers, the size of a box of cooking matches, can now readily be used to pump OSLs.^{33,140,156} Such pump lasers are slightly more sophisticated, short-pulse versions of green laser pointers.

Nevertheless, smaller, simpler, and cheaper sources are desirable. The microchip laser comprises a number of components: an infrared diode-pumped solid-state laser with a saturable absorber crystal to force a short pulsed mode of operation and a nonlinear crystal that frequency-doubles the laser to give a green output. To pump blue OSLs, a further nonlinear crystal is required to convert the pump source into the UV. Such systems require careful assembly of the multiple components for efficient output. The invention of blue InGaN diode lasers in 1996²⁷² and their subsequent

commercialization presents a potentially simpler alternative source for pumping OSLs. In the past few years, the output powers and lifetime of InGaN have substantially increased, particularly for wavelengths close to 410 nm. The recent convergence of InGaN maximum pulse energies with the lowest thresholds of OSLs has now led to the notable breakthrough of directly diode-pumped OSLs.^{49,220,221}

Several demonstrations of diode pumped OSLs based on conjugated polymers have recently been reported. Riedl et al. have demonstrated a tuneable blue-green laser based on a second-order polyfluorene DFB laser doped with a stilbene dye.⁴⁹ This laser was pumped with 50 ns pulses at 406 nm and had a threshold of 1.8 kW cm⁻², corresponding to a diode current of 400 mA. Karnutsch et al. have reported diode-pumped lasing in a polyfluorene first-order DFB laser.²²⁰ Vasdekis et al. have demonstrated lasing in short-cavity DBR lasers pumped with 1.2 ns pulses from a 407 nm diode laser.²²¹ They used an energy transfer gain medium with a coumarin laser dye host to efficiently harvest the diode light for a MEH-PPV guest emitter.

Such demonstrations are encouraging for the prospects of a further simplifying step, by using InGaN LEDs and even OLEDs as pump sources for OSLs. Such incoherent emitters could be directly integrated with the laser resonator, creating extremely compact, simple, and cheap visible lasers. There has also been recent progress in this area, with the successful integration of conjugated polymers and InGaN LEDs for visible wavelength conversion.^{273,274} InGaN micro-LEDs have been used to excite fluorescence in a range of polyfluorenes via both conventional photoluminescence²⁷³ and nonradiative Förster transfer.²⁷⁴ Tandem OLED structures, in which a small-molecule OLED excites photoluminescence in a parallel organic film has been reported to exhibit spatially coherent emission.²⁷⁵ While these integrated devices have only generated spontaneous emission to date, there are good prospects that they may be capable of stimulated emission. Hence although direct electrical pumping of OSLs is an extremely challenging problem, most of the benefits should be available in the near future via simple indirect pumping.

6. Conclusion

The field of easily processed organic semiconductor lasers (OSLs) is young at little more than a decade old and advancing rapidly. It provides exciting new challenges and opportunities for light-emitting materials beyond organic light-emitting diodes. There have been many important developments over the past few years. Laser and material design have advanced to reduce thresholds, enabling OSLs to be pumped by compact solid-state sources. Broad tuneability and simple fabrication have been shown as well as short pulse generation and broad-band optical amplification. These advances draw on well-known general features of organic semiconductors for any application, such as simple processing and the scope for tuning properties, and have stimulated work that exploits these properties in new ways. For example, the simple processing has enabled a remarkable range of laser structures to be made in very simple ways, including simple nanoimprinting of wavelength-scale features. In addition the scope for blending to tune properties has been used to reduce thresholds considerably. Some of the other advances draw on properties of the materials that are more specific to lasing, such as strong absorption and broad spectra, and use these properties in many ways. The strong absorption (and associated strong stimulated emission)

enables extraordinarily compact lasers and optical amplifiers to be made. The broad spectra enable not only tuneable lasers to be made but also femtosecond pulse generation and broad-band optical amplification. As we look to the future, it is important to keep in mind that this progress has been made mainly using materials developed for organic light-emitting diodes, so new opportunities and further progress can be expected from developing materials specifically for laser applications. Promising future directions include exploiting the compatibility with polymer optical fiber and using the distinctive chemical properties of organic semiconductors for sensing. Beyond that, electrical pumping remains a major challenge. However, a key recent breakthrough is the demonstration of direct optical pumping of polymer lasers by gallium nitride diode lasers. Such indirect electrical pumping gives many of the advantages of electrical pumping and paves the way for OSLs to become practical sources, initially for use in a range of spectroscopic applications.

Acknowledgments. We are grateful to the UK Engineering and Physical Sciences Research Council for financial support including an Advanced Research Fellowship (GAT) and a Senior Research Fellowship (IDWS).

7. References

- (1) Maiman, T. H. *Nature* **1960**, *187*, 493.
- (2) Dantus, M.; Bowman, R. M.; Zewail, A. H. *Nature* **1990**, *343*, 737.
- (3) Tsumura, A.; Koezuka, H.; Ando, T. *Appl. Phys. Lett.* **1986**, *49*, 1210.
- (4) Tang, C. W.; Vanslyke, S. A. *Appl. Phys. Lett.* **1987**, *51*, 913.
- (5) Burroughes, J. H.; Bradley, D. D. C.; Brown, A. R.; Marks, R. N.; Mackay, K.; Friend, R. H.; Burns, P. L.; Holmes, A. B. *Nature* **1990**, *347*, 539.
- (6) Knox, W. H.; Fork, R. L.; Downer, M. C.; Stolen, R. H.; Shank, C. V.; Valdmann, J. A. *Appl. Phys. Lett.* **1985**, *46*, 1120.
- (7) Soffer, B. H.; McFarland, B. B. *Appl. Phys. Lett.* **1967**, *10*, 266.
- (8) Karl, N. *Phys. Status Solidi A* **1972**, *13*, 651.
- (9) Avanesjan, O. S.; Benderskii, V. A.; Brikenstein, V. K.; Broude, V. L.; Korshunov, L. I.; Lavrushko, A. G.; Tartakovskii, II *Mol. Cryst. Liq. Cryst.* **1974**, *29*, 165.
- (10) Moses, D. *Appl. Phys. Lett.* **1992**, *60*, 3215.
- (11) Tessler, N.; Denton, G. J.; Friend, R. H. *Nature* **1996**, *382*, 695.
- (12) Hide, F.; DiazGarcia, M. A.; Schwartz, B. J.; Andersson, M. R.; Pei, Q. B.; Heeger, A. J. *Science* **1996**, *273*, 1833.
- (13) Holzer, W.; Penzkofer, A.; Gong, S. H.; Bleyer, A.; Bradley, D. D. C. *Adv. Mater.* **1996**, *8*, 974.
- (14) Frolov, S. V.; Ozaki, M.; Gellermann, W.; Vardeny, Z. V.; Yoshino, K. *Jpn. J. Appl. Phys., Part 2* **1996**, *35*, L1371.
- (15) Tessler, N. *Adv. Mater.* **1999**, *11*, 363.
- (16) Kozlov, V. G.; Forrest, S. R. *Curr. Opin. Solid State Mater. Sci.* **1999**, *4*, 203.
- (17) Kranzelbinder, G.; Leising, G. *Rep. Prog. Phys.* **2000**, *63*, 729.
- (18) McGehee, M. D.; Heeger, A. J. *Adv. Mater.* **2000**, *12*, 1655.
- (19) Scherf, U.; Riechel, S.; Lemmer, U.; Mahrt, R. F. *Curr. Opin. Solid State Mater. Sci.* **2001**, *5*, 143.
- (20) Samuel, I. D. W.; Turnbull, G. A. *Mater. Today* **2004**, *7*, 28.
- (21) Denton, G. J.; Tessler, N.; Stevens, M. A.; Friend, R. H. *Adv. Mater.* **1997**, *9*, 547.
- (22) DiazGarcia, M. A.; Hide, F.; Schwartz, B. J.; McGehee, M. D.; Andersson, M. R.; Heeger, A. J. *Appl. Phys. Lett.* **1997**, *70*, 3191.
- (23) Holzer, W.; Penzkofer, A.; Gong, S. H.; Davey, A. P.; Blau, W. J. *Opt. Quantum Electron.* **1997**, *29*, 713.
- (24) Schwartz, B. J.; Hide, F.; DiazGarcia, M. A.; Andersson, M. R.; Heeger, A. J. *Philos. Trans. R. Soc. London, Ser. A* **1997**, *355*, 775.
- (25) Gupta, R.; Stevenson, M.; Dogariu, A.; McGehee, M. D.; Park, J. Y.; Srdanov, V.; Heeger, A. J.; Wang, H. *Appl. Phys. Lett.* **1998**, *73*, 3492.
- (26) McGehee, M. D.; Diaz-Garcia, M. A.; Hide, F.; Gupta, R.; Miller, E. K.; Moses, D.; Heeger, A. J. *Appl. Phys. Lett.* **1998**, *72*, 1536.
- (27) Schulzgen, A.; Spiegelberg, C.; Morrell, M. M.; Mendes, S. B.; Kippelen, B.; Peyghambarian, N.; Nabor, M. F.; Mash, E. A.; Allemand, P. M. *Appl. Phys. Lett.* **1998**, *72*, 269.
- (28) Eradat, N.; Shkunov, M. N.; Frolov, S. V.; Gellermann, W.; Vardeny, Z. V.; Zakhidov, A. A.; Baughman, R. H.; Yoshino, K. *Synth. Met.* **1999**, *101*, 206.

- (29) Park, S. J.; Choi, E. S.; Oh, E. J.; Lee, K. W. *Mol. Cryst. Liq. Cryst.* **1999**, *337*, 97.
- (30) Shkunov, M. N.; Huang, J. D.; Vardeny, Z. V.; Yoshino, K. *Synth. Met.* **1999**, *102*, 1118.
- (31) Riechel, S.; Kallinger, C.; Lemmer, U.; Feldmann, J.; Gombert, A.; Wittwer, V.; Scherf, U. *Appl. Phys. Lett.* **2000**, *77*, 2310.
- (32) Turnbull, G. A.; Andrew, P.; Barnes, W. L.; Samuel, I. D. W. *Phys. Rev. B* **2003**, *67*, 165107.
- (33) Heliotis, G.; Xia, R.; Bradley, D. D. C.; Turnbull, G. A.; Samuel, I. D. W.; Andrew, P.; Barnes, W. L. *Appl. Phys. Lett.* **2003**, *83*, 2118.
- (34) Heliotis, G.; Bradley, D. D. C.; Turnbull, G. A.; Samuel, I. D. W. *Appl. Phys. Lett.* **2002**, *81*, 415.
- (35) Xia, R. D.; Heliotis, G.; Bradley, D. D. C. *Appl. Phys. Lett.* **2003**, *82*, 3599.
- (36) Theander, M.; Granlund, T.; Johanson, D. M.; Ruseckas, A.; Sundstrom, V.; Andersson, M. R.; Inganas, O. *Adv. Mater.* **2001**, *13*, 323.
- (37) Shkunov, M. N.; Osterbacka, R.; Fujii, A.; Yoshino, K.; Vardeny, Z. V. *Appl. Phys. Lett.* **1999**, *74*, 1648.
- (38) Lawrence, J. R.; Turnbull, G. A.; Samuel, I. D. W.; Richards, G. J.; Burn, P. L. *Opt. Lett.* **2004**, *29*, 869.
- (39) Wang, P. W.; Liu, Y. J.; Devadoss, C.; Bharathi, P.; Moore, J. S. *Adv. Mater.* **1996**, *8*, 237.
- (40) Halim, M.; Pillow, J. N. G.; Samuel, I. D. W.; Burn, P. L. *Synth. Met.* **1999**, *102*, 922.
- (41) Lo, S. C.; Anthopoulos, T. D.; Namdas, E. B.; Burn, P. L.; Samuel, I. D. W. *Adv. Mater.* **2005**, *17*, 1945.
- (42) Yokoyama, S.; Otomo, A.; Mashiko, S. *Appl. Phys. Lett.* **2002**, *80*, 7.
- (43) Otomo, A.; Yokoyama, S.; Nakahama, T.; Mashiko, S. *Appl. Phys. Lett.* **2000**, *77*, 3881.
- (44) Spehr, T.; Siebert, A.; Fuhrmann-Lieker, T.; Salbeck, J.; Rabe, T.; Riedl, T.; Johannes, H. H.; Kowalsky, W.; Wang, J.; Weimann, T.; Hinze, P. *Appl. Phys. Lett.* **2005**, *87*, 161103.
- (45) Xia, R.; Heliotis, G.; Campoy-Quiles, M.; Stavrinou, P. N.; Bradley, D. D. C.; Vak, D.; Kim, D. Y. *J. Appl. Phys.* **2005**, *98*, 083101.
- (46) Spehr, T.; Pudzich, R.; Fuhrmann, T.; Salbeck, J. *Org. Electron.* **2003**, *4*, 61.
- (47) Johansson, N.; Salbeck, J.; Bauer, J.; Weissortel, F.; Broms, P.; Andersson, A.; Salaneck, W. R. *Adv. Mater.* **1998**, *10*, 1136.
- (48) Dumarcher, V.; Rocha, L.; Denis, C.; Fiorini, C.; Nunzi, J. M.; Sobel, F.; Sahraoui, B.; Gindre, D. *J. Opt. A: Pure Appl. Opt.* **2000**, *2*, 279.
- (49) Riedl, T.; Rabe, T.; Johannes, H. H.; Kowalsky, W.; Wang, J.; Weimann, T.; Hinze, P.; Nehls, B.; Farrell, T.; Scherf, U. *Appl. Phys. Lett.* **2006**, *88*, 241116.
- (50) Schneider, D.; Rabe, T.; Riedl, T.; Dobbertin, T.; Werner, O.; Kroger, M.; Becker, E.; Johannes, H. H.; Kowalsky, W.; Weimann, T.; Wang, J.; Hinze, P.; Gerhard, A.; Stossel, P.; Vestweber, H. *Appl. Phys. Lett.* **2004**, *84*, 4693.
- (51) Sheridan, A. K.; Turnbull, G. A.; Safonov, A. N.; Samuel, I. D. W. *Phys. Rev. B* **2000**, *62*, 11929.
- (52) Turnbull, G. A.; Krauss, T. F.; Barnes, W. L.; Samuel, I. D. W. *Synth. Met.* **2001**, *121*, 1757.
- (53) Wegmann, G.; Giessen, H.; Greiner, A.; Mahrt, R. F. *Phys. Rev. B* **1998**, *57*, R4218.
- (54) Goossens, M.; Ruseckas, A.; Turnbull, G. A.; Samuel, I. D. W. *Appl. Phys. Lett.* **2004**, *85*, 31.
- (55) van den Berg, S. A.; van Schoonderwoerd den Bezemer, R. H.; Schoo, H. F. M.; 't Hooft, G. W.; Eliel, E. R. *Opt. Lett.* **1999**, *24*, 1847.
- (56) Goossens, M.; Heliotis, G.; Turnbull, G. A.; Ruseckas, A.; Lawrence, J. R.; Xia, R.; Bradley, D. D. C.; Samuel, I. D. W. In *Organic Light-Emitting Materials and Devices IX*; Kafafi, Z. H., Lane, P. A., Eds.; Proceedings of SPIE, The International Society for Optical Engineering, Vol. 5937; Society of Photo-Optical Instrumentation Engineers: Bellingham, WA, 2005; p 593706.
- (57) Amarasinghe, D.; Ruseckas, A.; Vasdekis, A. E.; Goossens, M.; Turnbull, G. A.; Samuel, I. D. W. *Appl. Phys. Lett.* **2006**, *89*, 201119.
- (58) deMello, J. C.; Wittmann, H. F.; Friend, R. H. *Adv. Mater.* **1997**, *9*, 230.
- (59) Greenham, N. C.; Burns, S. E.; Samuel, I. D. W.; Friend, R. H.; Moratti, S. C.; Holmes, A. B. *Mol. Cryst. Liq. Cryst. Sci. Technol., Sect. A* **1996**, *283*, 51.
- (60) Greenham, N. C.; Samuel, I. D. W.; Hayes, G. R.; Phillips, R. T.; Kessener, Y.; Moratti, S. C.; Holmes, A. B.; Friend, R. H. *Chem. Phys. Lett.* **1995**, *241*, 89.
- (61) Mattoussi, H.; Murata, H.; Merritt, C. D.; Iizumi, Y.; Kido, J.; Kafafi, Z. H. *J. Appl. Phys.* **1999**, *86*, 2642.
- (62) Pope, M.; Swenberg, C. E. *Electronic Processes in Organic Crystals and Polymers*; Oxford University Press: New York, 1999.
- (63) Tang, C. W.; Vanslyke, S. A.; Chen, C. H. *J. Appl. Phys.* **1989**, *65*, 3610.
- (64) Inganas, O.; Granlund, T.; Theander, M.; Berggren, M.; Andersson, M. R.; Ruseckas, A.; Sundstrom, V. *Opt. Mater.* **1998**, *9*, 104.
- (65) Halim, M.; Samuel, I. D. W.; Pillow, J. N. G.; Burn, P. L. *Synth. Met.* **1999**, *102*, 1113.
- (66) Salbeck, J.; Schorner, M.; Fuhrmann, T. *Thin Solid Films* **2002**, *417*, 20.
- (67) Siegman, A. E. *Lasers*; University Science Books: Sausalito, CA, 1986.
- (68) Svelto, O. *Principles of Lasers*, 4th ed.; Plenum Press: New York, 1998.
- (69) Rudenko, A. I.; Bassler, H. *Chem. Phys. Lett.* **1991**, *182*, 581.
- (70) Rauscher, U.; Bassler, H.; Bradley, D. D. C.; Hennecke, M. *Phys. Rev. B* **1990**, *42*, 9830.
- (71) Samuel, I. D. W.; Crystall, B.; Rumbles, G.; Burn, P. L.; Holmes, A. B.; Friend, R. H. *Synth. Met.* **1993**, *54*, 281.
- (72) Kersting, R.; Lemmer, U.; Mahrt, R. F.; Leo, K.; Kurz, H.; Bassler, H.; Gobel, E. O. *Phys. Rev. Lett.* **1993**, *70*, 3820.
- (73) Hayes, G. R.; Samuel, I. D. W.; Phillips, R. T. *Phys. Rev. B* **1995**, *52*, 11569.
- (74) Ruseckas, A.; Theander, M.; Valkunas, L.; Andersson, M. R.; Inganas, O.; Sundstrom, V. *J. Lumin.* **1998**, *76-77*, 474.
- (75) Berggren, M.; Dodabalapur, A.; Slusher, R. E. *Appl. Phys. Lett.* **1997**, *71*, 2230.
- (76) Kozlov, V. G.; Bulovic, V.; Burrows, P. E.; Forrest, S. R. *Nature* **1997**, *389*, 362.
- (77) Gupta, R.; Stevenson, M.; Heeger, A. J. *J. Appl. Phys.* **2002**, *92*, 4874.
- (78) Kozlov, V. G.; Bulovic, V.; Burrows, P. E.; Baldo, M.; Khalfin, V. B.; Parthasarathy, G.; Forrest, S. R.; You, Y.; Thompson, M. E. *J. Appl. Phys.* **1998**, *84*, 4096.
- (79) Dogariu, A.; Gupta, R.; Heeger, A. J.; Wang, H. *Synth. Met.* **1999**, *100*, 95.
- (80) Sheridan, A. K.; Buckley, A. R.; Fox, A. M.; Bacher, A.; Bradley, D. D. C.; Samuel, I. D. W. *J. Appl. Phys.* **2002**, *92*, 6367.
- (81) Brouwer, H. J.; Krasnikov, V. V.; Hilberer, A.; Wildeman, J.; Hadziioannou, G. *Appl. Phys. Lett.* **1995**, *66*, 3404.
- (82) Rabe, T.; Hoping, M.; Schneider, D.; Becker, E.; Johannes, H. H.; Kowalsky, W.; Weimann, T.; Wang, J.; Hinze, P.; Nehls, B. S.; Scherf, U.; Farrell, T.; Riedl, T. *Adv. Funct. Mater.* **2005**, *15*, 1188.
- (83) Samuel, I. D. W.; Raksi, F.; Bradley, D. D. C.; Friend, R. H.; Burn, P. L.; Holmes, A. B.; Murata, H.; Tsutsui, T.; Saito, S. *Synth. Met.* **1993**, *55*, 15.
- (84) Yan, M.; Rothberg, L. J.; Papadimitrakopoulos, F.; Galvin, M. E.; Miller, T. M. *Phys. Rev. Lett.* **1994**, *72*, 1104.
- (85) Denton, G. J.; Tessler, N.; Harrison, N. T.; Friend, R. H. *Phys. Rev. Lett.* **1997**, *78*, 733.
- (86) Kraabel, B.; Klimov, V. I.; Kohlman, R.; Xu, S.; Wang, H. L.; McBranch, D. W. *Phys. Rev. B* **2000**, *61*, 8501.
- (87) Frolov, S. V.; Vardeny, Z. V.; Yoshino, K. *Phys. Rev. B* **1998**, *57*, 9141.
- (88) Cerullo, G.; Stagira, S.; Nisoli, M.; De Silvestri, S.; Lanzani, G.; Krangelbinder, G.; Graupner, W.; Leising, G. *Phys. Rev. B* **1998**, *57*, 12806.
- (89) Shaklee, K. L.; Leheny, R. F. *Appl. Phys. Lett.* **1971**, *18*, 475.
- (90) de la Rosa-Fox, N. *Opt. Mater.* **1999**, *12*, 267.
- (91) McGehee, M. D.; Gupta, R.; Veenstra, S.; Miller, E. K.; Diaz-Garcia, M. A.; Heeger, A. J. *Phys. Rev. B* **1998**, *58*, 7035.
- (92) Jordan, G.; Flammich, M.; Ruther, M.; Kobayashi, T.; Blau, W. J.; Suzuki, Y.; Kaino, T. *Appl. Phys. Lett.* **2006**, *88*, 161114.
- (93) Berggren, M.; Dodabalapur, A.; Slusher, R. E.; Bao, Z. *Nature* **1997**, *389*, 466.
- (94) Kozlov, V. G.; Bulovic, V.; Forrest, S. R. *Appl. Phys. Lett.* **1997**, *71*, 2575.
- (95) Schafer, F. P. *Dye Lasers*, 3rd ed.; Springer-Verlag: Berlin, 1990.
- (96) Demartini, F.; Jacobovitz, G. R. *Phys. Rev. Lett.* **1988**, *60*, 1711.
- (97) Granlund, T.; Theander, M.; Berggren, M.; Andersson, M.; Ruseckas, A.; Sundstrom, V.; Bjork, G.; Granstrom, M.; Inganas, O. *Chem. Phys. Lett.* **1998**, *288*, 879.
- (98) Bulovic, V.; Kozlov, V. G.; Khalfin, V. B.; Forrest, S. R. *Science* **1998**, *279*, 553.
- (99) Horowitz, G. *J. Chim. Phys. Phys.-Chim. Biol.* **1998**, *95*, 1325.
- (100) Park, S. J.; Cho, I. H.; Lee, K. W. *Thin Solid Films* **2000**, *363*, 221.
- (101) Virgili, T.; Lidzey, D. G.; Grell, M.; Bradley, D. D. C.; Stagira, S.; Zavelani-Rossi, M.; De Silvestri, S. *Appl. Phys. Lett.* **2002**, *80*, 4088.
- (102) Lee, T. W.; Park, O. O.; Cho, H. N.; Kim, Y. C. *Opt. Mater.* **2003**, *21*, 673.
- (103) Koschorreck, M.; Gehlhaar, R.; Lyssenko, V. G.; Swoboda, M.; Hoffmann, M.; Leo, K. *Appl. Phys. Lett.* **2005**, *87*, 181108.
- (104) Persano, L.; Del Carro, P.; Mele, E.; Cingolani, R.; Pisignano, D.; Zavelani-Rossi, M.; Longhi, S.; Lanzani, G. *Appl. Phys. Lett.* **2006**, *88*, 121110.
- (105) Burns, S. E.; Denton, G.; Tessler, N.; Stevens, M. A.; Cacialli, F.; Friend, R. H. *Opt. Mater.* **1998**, *9*, 18.

- (106) Wu, D. J.; Wang, L. J.; Liu, Y.; Ning, Y. Q.; Zhao, J. M.; Liu, X. Y.; Wu, S. L.; He, X. D.; Lin, J. L.; Wang, L. X.; Ma, D. G.; Wang, D. K.; Jing, X. B.; Wang, F. S. *Synth. Met.* **2000**, *111*, 563.
- (107) Jewell, J. L.; Harbison, J. P.; Scherer, A.; Lee, Y. H.; Florez, L. T. *IEEE J. Quantum Electron.* **1991**, *27*, 1332.
- (108) Kuznetsov, M.; Hakimi, F.; Sprague, R.; Mooradian, A. *IEEE Photonics Technol. Lett.* **1997**, *9*, 1063.
- (109) Schulzgen, A.; Spiegelberg, C.; Morrell, M. M.; Mendes, S. B.; Allemand, P. M.; Kawabe, Y.; Kuwata-Gonokami, M.; Honkanen, S.; Fallahi, M.; Kippelen, B.; Peyghambarian, N. *Opt. Eng.* **1998**, *37*, 1149.
- (110) Stagira, S.; Zavelani-Rossi, M.; Nisoli, M.; DeSilvestri, S.; Lanzani, G.; Zenz, C.; Mataloni, P.; Leising, G. *Appl. Phys. Lett.* **1998**, *73*, 2860.
- (111) Zavelani-Rossi, M.; Lanzani, G.; De Silvestri, S.; Anni, M.; Gigli, G.; Cingolani, R.; Barbarella, G.; Favaretto, L. *Appl. Phys. Lett.* **2001**, *79*, 4082.
- (112) Fichou, D.; Delysse, S.; Nunzi, J. M. *Adv. Mater.* **1997**, *9*, 1178.
- (113) Zhu, X. H.; Gindre, D.; Mercier, N.; Frere, P.; Nunzi, J. M. *Adv. Mater.* **2003**, *15*, 906.
- (114) Ichikawa, M.; Hibino, R.; Inoue, M.; Haritani, T.; Hotta, S.; Araki, K.; Koyama, T.; Taniguchi, Y. *Adv. Mater.* **2005**, *17*, 2073.
- (115) Ichikawa, M.; Nakamura, K.; Inoue, M.; Mishima, H.; Haritani, T.; Hibino, R.; Koyama, T.; Taniguchi, Y. *Appl. Phys. Lett.* **2005**, *87*, 22113.
- (116) Shimizu, K.; Mori, Y.; Hotta, S. *J. Appl. Phys.* **2006**, *99*, 063505.
- (117) Kobayashi, T.; Blau, W. J. *Electron. Lett.* **2002**, *38*, 67.
- (118) Kobayashi, T.; Blau, W. J.; Tillmann, H.; Horhold, H. H. *IEEE J. Quantum Electron.* **2003**, *39*, 664.
- (119) Kobayashi, T.; Blau, W. J.; Tillmann, H.; Horhold, H. H. *J. Opt. A: Pure Appl. Opt.* **2002**, *4*, L1.
- (120) Frolov, S. V.; Shkunov, M.; Vardeny, Z. V.; Yoshino, K. *Phys. Rev. B* **1997**, *56*, R4363.
- (121) Frolov, S. V.; Vardeny, Z. V.; Yoshino, K. *Appl. Phys. Lett.* **1998**, *72*, 1802.
- (122) Kawabe, Y.; Spiegelberg, C.; Schulzgen, A.; Nabor, M. F.; Kippelen, B.; Mash, E. A.; Allemand, P. M.; Kuwata-Gonokami, M.; Takeda, K.; Peyghambarian, N. *Appl. Phys. Lett.* **1998**, *72*, 141.
- (123) Ramos-Ortiz, G.; Spiegelberg, C.; Peyghambarian, N.; Kippelen, B. *Appl. Phys. Lett.* **2000**, *77*, 2783.
- (124) Polson, R. C.; Levina, G.; Vardeny, Z. V. *Appl. Phys. Lett.* **2000**, *76*, 3858.
- (125) Osterbacka, R.; Wohlgenannt, M.; Shkunov, M.; Chinn, D.; Vardeny, Z. V. *J. Chem. Phys.* **2003**, *118*, 8905.
- (126) Yoshida, Y.; Nishimura, T.; Fujii, A.; Ozaki, M.; Yoshino, K. *Jpn. J. Appl. Phys., Part 2* **2005**, *44*, L1056.
- (127) Ben-Messaoud, T.; Dou, S. X.; Toussaere, E.; Potter, A.; Josse, D.; Kranzelbinder, G.; Zys, J. *Synth. Met.* **2002**, *127*, 159.
- (128) Fujii, A.; Frolov, S. V.; Vardeny, Z. V.; Yoshino, K. *Jpn. J. Appl. Phys., Part 2* **1998**, *37*, L740.
- (129) Berggren, M.; Dodabalapur, A.; Slusher, R. E.; Bao, Z. *Synth. Met.* **1997**, *91*, 65.
- (130) Frolov, S. V.; Fujii, A.; Chinn, D.; Hirohata, M.; Hidayat, R.; Taraguchi, M.; Masuda, T.; Yoshino, K.; Vardeny, Z. V. *Adv. Mater.* **1998**, *10*, 869.
- (131) Sheng, C. X.; Polson, R. C.; Vardeny, Z. V.; Chinn, D. A. *Synth. Met.* **2003**, *135*, 147.
- (132) Berggren, M.; Dodabalapur, A.; Bao, Z. N.; Slusher, R. E. *Adv. Mater.* **1997**, *9*, 968.
- (133) Frolov, S. V.; Shkunov, M.; Fujii, A.; Yoshino, K.; Vardeny, Z. V. *IEEE J. Quantum Electron.* **2000**, *36*, 2.
- (134) van den Berg, S. A.; Sautenkov, V. A.; 't Hooft, G. W.; Eliel, E. R. *Phys. Rev. A* **2002**, *65*, 053821.
- (135) van den Berg, S. A.; 't Hooft, G. W.; Eliel, E. R. *Chem. Phys. Lett.* **2001**, *347*, 167.
- (136) van den Berg, S. A.; 't Hooft, G. W.; Eliel, E. R. *Phys. Rev. A* **2001**, *63*, 063809.
- (137) Kumar, N. D.; Bhawalkar, J. D.; Prasad, P. N.; Karasz, F. E.; Hu, B. *Appl. Phys. Lett.* **1997**, *71*, 999.
- (138) Kumar, D. N.; Bhawalkar, J. D.; Prasad, P. N. *Appl. Opt.* **1998**, *37*, 510.
- (139) Kogelnik, H.; Shank, C. V. *J. Appl. Phys.* **1972**, *43*, 2327.
- (140) Turnbull, G. A.; Andrew, P.; Barnes, W. L.; Samuel, I. D. W. *Appl. Phys. Lett.* **2003**, *82*, 313.
- (141) Turnbull, G. A.; Andrew, P.; Jory, M. J.; Barnes, W. L.; Samuel, I. D. W. *Phys. Rev. B* **2001**, *64*, 125122.
- (142) Holzer, W.; Penzkofer, A.; Pertsch, T.; Danz, N.; Brauer, A.; Kley, E. B.; Tillmann, H.; Bader, C.; Horhold, H. H. *Appl. Phys. B: Lasers Opt.* **2002**, *74*, 333.
- (143) Andrew, P.; Turnbull, G. A.; Samuel, I. D. W.; Barnes, W. L. *Appl. Phys. Lett.* **2002**, *81*, 954.
- (144) Matsui, T.; Ozaki, M.; Yoshino, K.; Kajzar, F. *Jpn. J. Appl. Phys., Part 2* **2002**, *41*, L1386.
- (145) Heliotis, G.; Xia, R. D.; Turnbull, G. A.; Andrew, P.; Barnes, W. L.; Samuel, I. D. W.; Bradley, D. D. C. *Adv. Funct. Mater.* **2004**, *14*, 91.
- (146) Xia, R.; Heliotis, G.; Stavrinou, P. N.; Bradley, D. D. C. *Appl. Phys. Lett.* **2005**, *87*, 031104.
- (147) Heliotis, G.; Choulis, S. A.; Itskos, G.; Xia, R.; Murray, R.; Stavrinou, P. N.; Bradley, D. D. C. *Appl. Phys. Lett.* **2006**, *88*, 081104.
- (148) Karnutsch, C.; Gyrtner, C.; Haug, V.; Lemmer, U.; Farrell, T.; Nehls, B. S.; Scherf, U.; Wang, J.; Weimann, T.; Heliotis, G.; Pflumm, C.; deMello, J. C.; Bradley, D. D. C. *Appl. Phys. Lett.* **2006**, *89*, 201108.
- (149) Kallinger, C.; Hilmer, M.; Haugeneder, A.; Perner, M.; Spirkl, W.; Lemmer, U.; Feldmann, J.; Scherf, U.; Mullen, K.; Gombert, A.; Wittwer, V. *Adv. Mater.* **1998**, *10*, 920.
- (150) Riechel, S.; Lemmer, U.; Feldmann, J.; Benstem, T.; Kowalsky, W.; Scherf, U.; Gombert, A.; Wittwer, V. *Appl. Phys. B: Lasers Opt.* **2000**, *71*, 897.
- (151) Reufer, M.; Riechel, S.; Lupton, J. M.; Feldmann, J.; Lemmer, U.; Schneider, D.; Benstem, T.; Dobbertin, T.; Kowalsky, W.; Gombert, A.; Forberich, K.; Wittwer, V.; Scherf, U. *Appl. Phys. Lett.* **2004**, *84*, 3262.
- (152) Forberich, K.; Gombert, A.; Pereira, S.; Crewett, J.; Lemmer, U.; Diem, M.; Busch, K. *J. Appl. Phys.* **2006**, *100*, 023110.
- (153) Forberich, K.; Diem, M.; Crewett, J.; Lemmer, U.; Gombert, A.; Busch, K. *Appl. Phys. B: Lasers Opt.* **2006**, *82*, 539.
- (154) Berggren, M.; Dodabalapur, A.; Slusher, R. E.; Timko, A.; Nalamasu, O. *Appl. Phys. Lett.* **1998**, *72*, 410.
- (155) Dodabalapur, A.; Berggren, M.; Slusher, R. E.; Bao, Z.; Timko, A.; Schiortino, P.; Laskowski, E.; Katz, H. E.; Nalamasu, O. *IEEE J. Sel. Top. Quantum Electron.* **1998**, *4*, 67.
- (156) Riechel, S.; Lemmer, U.; Feldmann, J.; Berleb, S.; Muckl, A. G.; Brutting, W.; Gombert, A.; Wittwer, V. *Opt. Lett.* **2001**, *26*, 593.
- (157) Pisignano, D.; Anni, M.; Gigli, G.; Cingolani, R.; Barbarella, G.; Favaretto, L.; Sotgiu, G. B. V. *Synth. Met.* **2003**, *137*, 1057.
- (158) Pisignano, D.; Persano, L.; Visconti, P.; Cingolani, R.; Gigli, G.; Barbarella, G.; Favaretto, L. *Appl. Phys. Lett.* **2003**, *83*, 2545.
- (159) Schneider, D.; Hartmann, S.; Benstem, T.; Dobbertin, T.; Heithecker, D.; Metzendorf, D.; Becker, E.; Riedl, T.; Johannes, H. H.; Kowalsky, W.; Weimann, T.; Wang, J.; Hinze, P. *Appl. Phys. B: Lasers Opt.* **2003**, *77*, 399.
- (160) Pisignano, D.; Persano, L.; Mele, E.; Visconti, P.; Anni, M.; Gigli, G.; Cingolani, R.; Favaretto, L.; Barbarella, G. *Synth. Met.* **2005**, *153*, 237.
- (161) Schneider, D.; Rabe, T.; Riedl, T.; Dobbertin, T.; Kroger, M.; Becker, E.; Johannes, H. H.; Kowalsky, W.; Weimann, T.; Wang, J.; Hinze, P. *J. Appl. Phys.* **2005**, *98*, 043104.
- (162) Pisignano, D.; Persano, L.; Mele, E.; Visconti, P.; Cingolani, R.; Gigli, G.; Barbarella, G.; Favaretto, L. *Opt. Lett.* **2005**, *30*, 260.
- (163) Kozlov, V. G.; Parthasarathy, G.; Burrows, P. E.; Khalif, V. B.; Wang, J.; Chou, S. Y.; Forrest, S. R. *IEEE J. Quantum Electron.* **2000**, *36*, 18.
- (164) Schneider, D.; Rabe, T.; Riedl, T.; Dobbertin, T.; Kroger, M.; Becker, E.; Johannes, H. H.; Kowalsky, W.; Weimann, T.; Wang, J.; Hinze, P. *Appl. Phys. Lett.* **2004**, *85*, 1659.
- (165) Schneider, D.; Rabe, T.; Riedl, T.; Dobbertin, T.; Kroger, M.; Becker, E.; Johannes, H. H.; Kowalsky, W.; Weimann, T.; Wang, J.; Hinze, P.; Gerhard, A.; Stossel, P.; Vestweber, H. *Adv. Mater.* **2005**, *17*, 31.
- (166) Gupta, R.; Stevenson, M.; McGehee, M. D.; Dogariu, A.; Srdanov, V.; Park, J. Y.; Heeger, A. J. *Synth. Met.* **1999**, *102*, 875.
- (167) Xia, R. D.; Heliotis, G.; Hou, Y. B.; Bradley, D. D. C. *Org. Electron.* **2003**, *4*, 165.
- (168) Rose, A.; Zhu, Z. G.; Madigan, C. F.; Swager, T. M.; Bulovic, V. *Nature* **2005**, *434*, 876.
- (169) Turnbull, G. A.; Andrew, P.; Jory, M. J.; Barnes, W. L.; Samuel, I. D. W. *Synth. Met.* **2002**, *127*, 45.
- (170) Suzuki, K.; Takahashi, K.; Seida, Y.; Shimizu, K.; Kumagai, M.; Taniguchi, Y. *Jpn. J. Appl. Phys., Part 2* **2003**, *42*, L249.
- (171) Heliotis, G.; Xia, R.; Bradley, D. D. C.; Turnbull, G. A.; Samuel, I. D. W.; Andrew, P.; Barnes, W. L. *J. Appl. Phys.* **2004**, *96*, 6959.
- (172) Schneider, D.; Rabe, T.; Riedl, T.; Dobbertin, T.; Kroger, M.; Becker, E.; Johannes, H. H.; Kowalsky, W.; Weimann, T.; Wang, J.; Hinze, P. *Appl. Phys. Lett.* **2004**, *85*, 1886.
- (173) Stehr, J.; Crewett, J.; Schindler, F.; Sperling, R.; von Plessen, G.; Lemmer, U.; Lupton, J. M.; Klar, T. A.; Feldmann, J.; Holleitner, A. W.; Forster, M.; Scherf, U. *Adv. Mater.* **2003**, *15*, 1726.
- (174) Lawrence, J. R.; Turnbull, G. A.; Samuel, I. D. W. *Appl. Phys. Lett.* **2003**, *82*, 4023.
- (175) Vasdekis, A. E.; Turnbull, G. A.; Samuel, I. D. W.; Andrew, P.; Barnes, W. L. *Appl. Phys. Lett.* **2005**, *86*, 161102.
- (176) Notomi, M.; Suzuki, H.; Tamamura, T. *Appl. Phys. Lett.* **2001**, *78*, 1325.
- (177) Bauer, C.; Giessen, H.; Schnabel, B.; Kley, E. B.; Schmitt, C.; Scherf, U.; Mahrt, R. F. *Adv. Mater.* **2001**, *13*, 1161.

- (178) Moll, N.; Mahrt, R. F.; Bauer, C.; Giessen, H.; Schnabel, B.; Kley, E. B.; Scherf, U. *Appl. Phys. Lett.* **2002**, *80*, 734.
- (179) Barlow, G. F.; Shore, A.; Turnbull, G. A.; Samuel, I. D. W. *J. Opt. Soc. Am. B* **2004**, *21*, 2142.
- (180) Jebali, A.; Mahrt, R. F.; Moll, N.; Erni, D.; Bauer, C.; Bona, G. L.; Bachtold, W. *J. Appl. Phys.* **2004**, *96*, 3043.
- (181) Turnbull, G. A.; Carleton, A.; Barlow, G. F.; Tahraoui, A.; Krauss, T. F.; Shore, K. A.; Samuel, I. D. W. *J. Appl. Phys.* **2005**, *98*, 023105.
- (182) Turnbull, G. A.; Carleton, A.; Tahraoui, A.; Krauss, T. F.; Samuel, I. D. W.; Barlow, G. F.; Shore, K. A. *Appl. Phys. Lett.* **2005**, *87*.
- (183) Notomi, M.; Suzuki, H.; Tamamura, T.; Edagawa, K. *Phys. Rev. Lett.* **2004**, *92*, 123906.
- (184) Polson, R. C.; Chipouline, A.; Vardeny, Z. V. *Adv. Mater.* **2001**, *13*, 760.
- (185) Polson, R. C.; Raikh, M. E.; Vardeny, Z. V. *Phys. E (Amsterdam, Neth.)* **2002**, *13*, 1240.
- (186) Anni, M.; Lattante, S.; Cingolani, R.; Gigli, G.; Barbarella, G.; Favaretto, L. *Appl. Phys. Lett.* **2003**, *83*, 2754.
- (187) Quochi, F.; Cordella, F.; Orru, R.; Communal, J. E.; Verzeroli, P.; Mura, A.; Bongiovanni, G.; Andreev, A.; Sitter, H.; Sariciftci, N. S. *Appl. Phys. Lett.* **2004**, *84*, 4454.
- (188) Quochi, F.; Cordella, F.; Mura, A.; Bongiovanni, G.; Balzer, F.; Rubahn, H. G. *Appl. Phys. Lett.* **2006**, *88*, 041106.
- (189) Yoshino, K.; Tatsuura, S.; Kawagishi, Y.; Ozaki, M.; Zakhidov, A. A.; Vardeny, Z. V. *Appl. Phys. Lett.* **1999**, *74*, 2590.
- (190) Eradat, N.; Wohlgenannt, M.; Vardeny, Z. V.; Zakhidov, A. A.; Baughman, R. H. *Synth. Met.* **2001**, *116*, 509.
- (191) Hide, F.; Schwartz, B. J.; DiazGarcia, M. A.; Heeger, A. J. *Chem. Phys. Lett.* **1996**, *256*, 424.
- (192) Polson, R. C.; Vardeny, Z. V. *Phys. B (Amsterdam, Neth.)* **2003**, *338*, 219.
- (193) Polson, R. C.; Vardeny, Z. V. *Phys. Rev. B* **2005**, *71*, 045205.
- (194) Yablonovitch, E. *J. Opt. Soc. Am. B* **1993**, *10*, 283.
- (195) Meier, M.; Mekis, A.; Dodabalapur, A.; Timko, A.; Slusher, R. E.; Joannopoulos, J. D.; Nalamasu, O. *Appl. Phys. Lett.* **1999**, *74*, 7.
- (196) Barlow, G. F.; Shore, K. A. *IEEE Proc.-Optoelectron.* **2001**, *148*, 2.
- (197) Kretsch, K. P.; Blau, W. J.; Dumarcher, V.; Rocha, L.; Fiorini, C.; Nunzi, J. M.; Pfeiffer, S.; Tillmann, H.; Horhold, H. H. *Appl. Phys. Lett.* **2000**, *76*, 2149.
- (198) Tsutsumi, N.; Fujihara, A. *Appl. Phys. Lett.* **2005**, *86*, 061101.
- (199) Tsutsumi, N.; Fujihara, A.; Hayashi, D. *Appl. Opt.* **2006**, *45*, 5748.
- (200) Tsutsumi, N.; Kawahira, T.; Sakai, W. *Appl. Phys. Lett.* **2003**, *83*, 2533.
- (201) Tsutsumi, N.; Yamamoto, M. *J. Opt. Soc. Am. B* **2006**, *23*, 842.
- (202) Sobel, F.; Gindre, D.; Nunzi, J. M.; Denis, C.; Dumarcher, V.; Fiorini-Debuisschert, C.; Kretsch, K. P.; Rocha, L. *Opt. Mater.* **2004**, *27*, 199.
- (203) Kranzelbinder, G.; Toussaere, E.; Zyss, J.; Pogantsch, A.; List, E. W. J.; Tillmann, H.; Horhold, H. H. *Appl. Phys. Lett.* **2002**, *80*, 716.
- (204) Maillou, T.; Le Moigne, J.; Dumarcher, V.; Rocha, L.; Geffroy, B.; Nunzi, J. M. *Adv. Mater.* **2002**, *14*, 1297.
- (205) Baldo, M.; Deutsch, M.; Burrows, P.; Gossenberger, H.; Gerstenberg, M.; Ban, V.; Forrest, S. *Adv. Mater.* **1998**, *10*, 1505.
- (206) Heliotis, G.; Xia, R.; Whitehead, K. S.; Turnbull, G. A.; Samuel, I. D. W.; Bradley, D. D. C. *Synth. Met.* **2003**, *139*, 727.
- (207) Xia, R. D.; Campoy-Quiles, M.; Heliotis, G.; Stavrinou, P.; Whitehead, K. S.; Bradley, D. D. C. *Synth. Met.* **2005**, *155*, 274.
- (208) Anni, M.; Gigli, G.; Cingolani, R.; Patane, S.; Arena, A.; Allegrini, M. *Appl. Phys. Lett.* **2001**, *79*, 1381.
- (209) Lawrence, J. R.; Andrew, P.; Barnes, W. L.; Buck, M.; Turnbull, G. A.; Samuel, I. D. W. *Appl. Phys. Lett.* **2002**, *81*, 1955.
- (210) Meier, M.; Dodabalapur, A.; Rogers, J. A.; Slusher, R. E.; Mekis, A.; Timko, A.; Murray, C. A.; Ruel, R.; Nalamasu, O. *J. Appl. Phys.* **1999**, *86*, 3502.
- (211) Pisignano, D.; Mele, E.; Persano, L.; Gigli, G.; Visconti, P.; Cingolani, R.; Barbarella, G.; Favaretto, L. *Phys. Rev. B* **2004**, *70*, 205206.
- (212) Rogers, J. A.; Meier, M.; Dodabalapur, A.; Laskowski, E. J.; Cappuzzo, M. A. *Appl. Phys. Lett.* **1999**, *74*, 3257.
- (213) Ichikawa, M.; Tanaka, Y.; Suganuma, N.; Koyama, T.; Taniguchi, Y. *Jpn. J. Appl. Phys., Part 1* **2003**, *42*, 5590.
- (214) Pisignano, D.; Persano, L.; Raganato, M. F.; Visconti, P.; Cingolani, R.; Barbarella, G.; Favaretto, L.; Gigli, G. *Adv. Mater.* **2004**, *16*, 525.
- (215) Suzuki, H.; Yokoo, A.; Notomi, M. *Polym. Adv. Technol.* **2004**, *15*, 75.
- (216) Pisignano, D.; Persano, L.; Cingolani, R.; Gigli, G.; Babudri, F.; Farinola, G. M.; Naso, F. *Appl. Phys. Lett.* **2004**, *84*, 1365.
- (217) Pisignano, D.; Mele, E.; Persano, L.; Paladini, G.; Cingolani, R. *Appl. Phys. Lett.* **2005**, *86*, 261104.
- (218) Sims, M.; Zheng, K.; Quiles, M. C.; Xia, R.; Stavrinou, P. N.; Bradley, D. D. C.; Etchegoin, P. *J. Phys.: Condens. Matter* **2005**, *17*, 6307.
- (219) Gaal, M.; Gadermaier, C.; Plank, H.; Moderegger, E.; Pogantsch, A.; Leising, G.; List, E. J. W. *Adv. Mater.* **2003**, *15*, 1165.
- (220) Karnutsch, C.; Haug, V.; Gaertner, C.; Lemmer, U.; Farrell, T.; Nehls, B.; Scherf, U.; Wang, J.; Weimann, T.; Heliotis, G.; Pflumm, C.; DeMello, J.; Bradley, D. D. C. Presented at the Conference on Lasers and Optoelectronics 2006, Long Beach, 2006; p CFJ3.
- (221) Vasdekis, A. E.; Tsiminis, G.; Ribierre, J.-C.; O'Faolain, L.; Krauss, T. F.; Turnbull, G. A.; Samuel, I. D. W. *Opt. Express* **2006**, *14*, 9211.
- (222) Coldren, L. A.; Corzine, S. W. *Diode Lasers and Photonic Integrated Circuits*; Wiley: New York, 1995.
- (223) Zavelani-Rossi, M.; Perissinotto, S.; Lanzani, G.; Salerno, M.; Gigli, G. *Appl. Phys. Lett.* **2006**, *89*.
- (224) Rabe, T.; Gerlach, K.; Riedl, T.; Johannes, H.-H.; Kowalsky, W.; Niederhofer, J.; Gries, W.; Wang, J.; Weimann, T.; Hinze, P.; Galbrecht, F.; Scherf, U. *Appl. Phys. Lett.* **2006**, *89*, 081115.
- (225) Bornemann, R.; Lemmer, U.; Thiel, E. *Opt. Lett.* **2006**, *31*, 1669.
- (226) Chandra, S.; Allik, T. H.; Hutchinson, J. A.; Fox, J.; Swim, C. *Opt. Lett.* **1997**, *22*, 209.
- (227) Guggel, H. P.; Artmann, H.; Geng, C.; Scholz, F.; Schweizer, P. *IEEE Photonics Technol. Lett.* **1997**, *9*, 14.
- (228) Kobayashi, T.; Savatier, J. B.; Jordan, G.; Blau, W. J.; Suzuki, Y.; Kaino, T. *Appl. Phys. Lett.* **2004**, *85*, 185.
- (229) Wong, W. H.; Pun, E. Y. B.; Chan, K. S. *Appl. Phys. Lett.* **2004**, *84*, 176.
- (230) Tessler, N.; Medvedev, V.; Kazes, M.; Kan, S. H.; Banin, U. *Science* **2002**, *295*, 1506.
- (231) Solomeshch, O.; Kigel, A.; Saschiuk, A.; Medvedev, V.; Aharoni, A.; Razin, A.; Eichen, Y.; Banin, U.; Lifshitz, E.; Tessler, N. *J. Appl. Phys.* **2005**, *98*, 074310.
- (232) Verdaasdonk, R. M.; vanSwol, C. F. P. *Phys. Med. Biol.* **1997**, *42*, 869.
- (233) Ntziachristos, V.; Bremer, C.; Weissleder, R. *Eur. Radiol.* **2003**, *13*, 195.
- (234) Miyai, E.; Sakai, K.; Okano, T.; Kunishi, W.; Ohnishi, D.; Noda, S. *Nature* **2006**, *441*, 946.
- (235) Oki, Y.; Miyamoto, S.; Maeda, M.; Vasa, N. J. *Opt. Lett.* **2002**, *27*, 1220.
- (236) Balslev, S.; Jorgensen, A. M.; Bilenberg, B.; Mogensen, K. B.; Snakenborg, D.; Geschke, O.; Kutter, J. P.; Kristensen, A. *Lab Chip* **2006**, *6*, 213.
- (237) Zubia, J.; Arrue, J. *Opt. Fiber Technol.* **2001**, *7*, 101.
- (238) Ma, H.; Jen, A. K. Y.; Dalton, L. R. *Adv. Mater.* **2002**, *14*, 1339.
- (239) Lawrence, J. R.; Turnbull, G. A.; Samuel, I. D. W. *Appl. Phys. Lett.* **2002**, *80*, 3036.
- (240) Heliotis, G.; Bradley, D. D. C.; Goossens, M.; Richardson, S.; Turnbull, G. A.; Samuel, I. D. W. *Appl. Phys. Lett.* **2004**, *85*, 6122.
- (241) Wong, W. H.; Chan, K. S.; Pun, E. Y. B. *Appl. Phys. Lett.* **2005**, *87*, 011103.
- (242) Frolov, S. V.; Liess, M.; Lane, P. A.; Gellermann, W.; Vardeny, Z. V.; Ozaki, M.; Yoshino, K. *Phys. Rev. Lett.* **1997**, *78*, 4285.
- (243) Virgili, T.; Marinotto, D.; Lanzani, G.; Bradley, D. D. C. *Appl. Phys. Lett.* **2005**, *86*, 091113.
- (244) McQuade, D. T.; Pullen, A. E.; Swager, T. M. *Chem. Rev.* **2000**, *100*, 2537.
- (245) Yang, J. S.; Swager, T. M. *J. Am. Chem. Soc.* **1998**, *120*, 11864.
- (246) Cumming, C. J.; Aker, C.; Fisher, M.; Fox, M.; la Grone, M. J.; Reust, D.; Rockley, M. G.; Swager, T. M.; Towers, E.; Williams, V. *IEEE Trans. Geosci. Remote Sensing* **2001**, *39*, 1119.
- (247) Ho, H. A.; Boissinot, M.; Bergeron, M. G.; Corbeil, G.; Dore, K.; Boudreau, D.; Leclerc, M. *Angew. Chem., Int. Ed.* **2002**, *41*, 1548.
- (248) Ho, H. A.; Dore, K.; Boissinot, M.; Bergeron, M. G.; Tanguay, R. M.; Boudreau, D.; Leclerc, M. *J. Am. Chem. Soc.* **2005**, *127*, 12673.
- (249) Gaylord, B. S.; Heeger, A. J.; Bazan, G. C. *J. Am. Chem. Soc.* **2003**, *125*, 896.
- (250) Kim, I. B.; Erdogan, B.; Wilson, J. N.; Bunz, U. H. F. *Chem.—Eur. J.* **2004**, *10*, 6247.
- (251) Nilsson, K. P. R.; Ingnas, O. *Macromolecules* **2004**, *37*, 9109.
- (252) Tang, Y. L.; He, F.; Yu, M. H.; Feng, F. D.; An, L. L.; Sun, H.; Wang, S.; Li, Y. L.; Zhu, D. B. *Macromol. Rapid Commun.* **2006**, *27*, 389.
- (253) Schon, J. H.; Kloc, C.; Dodabalapur, A.; Batlogg, B. *Science* **2000**, *289*, 599.
- (254) El-Nadi, L.; Al-Houty, L.; Omar, M. M.; Ragab, M. *Chem. Phys. Lett.* **1998**, *286*, 9.
- (255) Schon, J. H.; Kloc, C.; Dodabalapur, A.; Batlogg, B. *Science* **2002**, *298*, 961.
- (256) Redecker, M.; Bradley, D. D. C.; Inbasekaran, M.; Woo, E. P. *Appl. Phys. Lett.* **1998**, *73*, 1565.
- (257) Tessler, N.; Harrison, N. T.; Friend, R. H. *Adv. Mater.* **1998**, *10*, 64.
- (258) Yamamoto, H.; Kasajima, H.; Yokoyama, W.; Sasabe, H.; Adachi, C. *Appl. Phys. Lett.* **2005**, *86*, 083502.
- (259) Matsushima, T.; Sasabe, H.; Adachi, C. *Appl. Phys. Lett.* **2006**, *88*, 033508.

- (260) Yamamoto, H.; Oyamada, T.; Sasabe, H.; Adachi, C. *Appl. Phys. Lett.* **2004**, *84*, 1401.
- (261) Samuel, I. D. W. *Nature* **2004**, *429*, 709.
- (262) Zaumseil, J.; Friend, R. H.; Sirringhaus, H. *Nat. Mater.* **2006**, *5*, 69.
- (263) Rost, C.; Karg, S.; Riess, W.; Loi, M. A.; Murgia, M.; Muccini, M. *Appl. Phys. Lett.* **2004**, *85*, 1613.
- (264) Sakanoue, T.; Fujiwara, E.; Yamada, R.; Tada, H. *Appl. Phys. Lett.* **2004**, *84*, 3037.
- (265) Ahles, M.; Hepp, A.; Schmechel, R.; von Seggern, H. *Appl. Phys. Lett.* **2004**, *84*, 428.
- (266) Pauchard, M.; Swensen, J.; Moses, D.; Heeger, A. J.; Perzon, E.; Andersson, M. R. *J. Appl. Phys.* **2003**, *94*, 3543.
- (267) Oyamada, T.; Sasabe, H.; Adachi, C.; Okuyama, S.; Shimoji, N.; Matsushige, K. *Appl. Phys. Lett.* **2005**, *86*, 093505.
- (268) Baldo, M. A.; Holmes, R. J.; Forrest, S. R. *Phys. Rev. B* **2002**, *66*, 035321.
- (269) Pflumm, C.; Karnutsch, C.; Gerken, M.; Lemmer, U. *IEEE J. Quantum Electron.* **2005**, *41*, 316.
- (270) Gaertner, C.; Pflumm, C.; Karnutsch, C.; Houg, V.; Lemmer, U. *Proc. SPIE* **2006**, *6333*, 63331J.
- (271) Pflumm, C.; Gaertner, C.; Karnutsch, C.; Lemmer, U. *Proc. SPIE* **2006**, *6333*, 63330W.
- (272) Nakamura, S.; Senoh, M.; Nagahama, S.; Iwasa, N.; Yamada, T.; Matsushita, T.; Kiyoku, H.; Sugimoto, Y. *Jpn. J. Appl. Phys., Part 2* **1996**, *35*, L74.
- (273) Heliotis, G.; Gu, E.; Griffin, C.; Jeon, C. W.; Stavrinou, P. N.; Dawson, M. D.; Bradley, D. D. C. *J. Opt. A: Pure Appl. Opt.* **2006**, *8*, S445.
- (274) Heliotis, G.; Itskos, G.; Murray, R.; Dawson, M. D.; Watson, I. M.; Bradley, D. D. C. *Adv. Mater.* **2006**, *18*, 334.
- (275) Duarte, F. J.; Liao, L. S.; Vaeth, K. M. *Opt. Lett.* **2005**, *30*, 3072.

CR050152I